



Published in final edited form as:

*Photochem Photobiol.* 2020 March ; 96(2): 232–259. doi:10.1111/php.13209.

## Photodynamic Therapy and the Biophysics of the Tumor Microenvironment†

**Aaron J. Sorrin<sup>1,θ</sup>, Mustafa Kemal Ruhi<sup>2,θ</sup>, Nathaniel A. Ferlic<sup>3</sup>, Vida Karimnia<sup>4</sup>, William J. Polacheck<sup>2,6,7</sup>, Jonathan P. Celli<sup>4</sup>, Huang-Chiao Huang<sup>1,5,#</sup>, Imran Rizvi<sup>2,7,#</sup>**

<sup>1</sup>Fischell Department of Bioengineering, University of Maryland, College Park, MD, 20742, USA

<sup>2</sup>Joint Department of Biomedical Engineering, University of North Carolina at Chapel Hill, Chapel Hill, NC and North Carolina State University, Raleigh, NC, 27599, USA

<sup>3</sup>Department of Electrical and Computer Engineering, University of Maryland, College Park, MD, 20742, USA

<sup>4</sup>Department of Physics, College of Science and Mathematics, University of Massachusetts at Boston, Boston, MA, 02125, USA

<sup>5</sup>Marlene and Stewart Greenebaum Cancer Center, University of Maryland School of Medicine, Baltimore, MD 21201, USA

<sup>6</sup>Department of Cell Biology and Physiology, University of North Carolina School of Medicine, Chapel Hill, NC 27599, USA

<sup>7</sup>Lineberger Comprehensive Cancer Center, University of North Carolina School of Medicine, Chapel Hill, NC, 27599, USA

### Abstract

Targeting the tumor microenvironment (TME) provides opportunities to modulate tumor physiology, enhance the delivery of therapeutic agents, impact immune response, and overcome resistance. Photodynamic therapy (PDT) is a photochemistry-based, non-thermal modality that produces reactive molecular species at the site of light activation and is in the clinic for non-oncologic and oncologic applications. The unique mechanisms, and exquisite spatiotemporal control, inherent to PDT enable selective modulation or destruction of the TME and cancer cells. Mechanical stress plays an important role in tumor growth and survival, with increasing implications for therapy design and drug delivery, but remains understudied in the context of PDT and PDT-based combinations. This review describes pharmacoengineering and bioengineering approaches in PDT to target cellular and non-cellular components of the TME, as well as molecular targets on tumor and tumor-associated cells. Particular emphasis is placed on the role of mechanical stress in the context of targeted PDT regimens, and combinations, for primary and metastatic tumors.

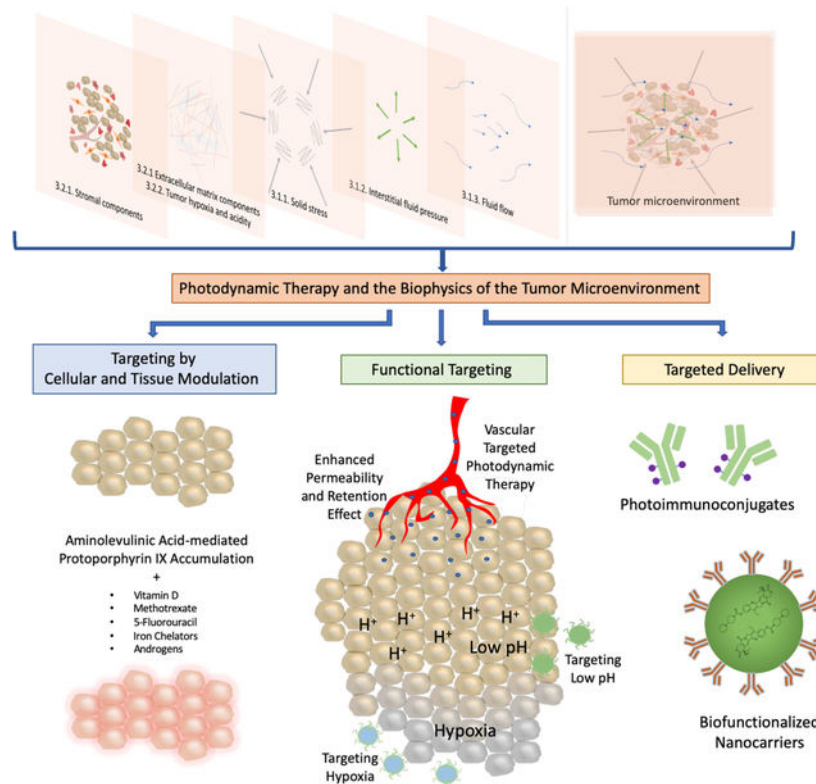
†This article is part of a Special Issue dedicated to Dr. Jarod Finlay.

\*Corresponding authors: imran.rizvi@unc.edu (Imran Rizvi) and hchuang@umd.edu (Huang-Chiao Huang).

<sup>θ</sup>equal contribution

<sup>#</sup>equal contribution

## Graphical Abstract



Physical stress in the tumor microenvironment impacts actionable targets for photodynamic therapy-based regimens. The design of targeted photodynamic therapy approaches, and rational combinations, that exploit and modulate mechanical stress and stromal components in the tumor microenvironment are discussed in this review.

## INTRODUCTION

Photodynamic therapy (PDT) is a light-based treatment modality that involves electronic excitation of a photosensitizer (PS) to mediate the production of reactive molecular species and induce photodamage at the site of light activation (1–3). PDT provides unique cytotoxic mechanisms and exquisite spatiotemporal control, which makes it an attractive approach to directly target tumor cells and/or the tumor microenvironment (TME, Figure 1). Depending, in part, on the localization of the PS, PDT can directly damage or alter targets in tumor cells such as mitochondrial function, pro-survival pathways, antioxidative effects, efflux transporters, and stimulators of immune response. These topics, and their implications for PDT-based regimens, have been discussed in many excellent articles and reviews (4–11), but are largely outside the scope of the current article. The focus of this review is on physical stress in the TME and implications for the design of targeted PDT approaches and combinations. Major components of the TME are introduced with a focus on mechanical stress. Three categories of targeted PDT that exploit cellular, molecular and mechanical

features in the TME are discussed: I) targeting by cellular and tissue modulation, II) functional targeting and III) targeted delivery (Figure 2).

Targeting by cellular and tissue modulation refers to strategies that manipulate cell metabolism to regulate photosensitizer (PS) production and response to treatment (12). For example, a pro-drug, 5-aminolevulinic acid (5-ALA), can be enzymatically converted into the PS, protoporphyrin (PpIX), through the heme biosynthetic pathway. Much of the research in cellular and tissue modulation to enhance PDT efficacy involves manipulating the rate-limiting steps that convert 5-ALA into heme to increase intracellular PpIX concentrations (12). A recent study examining the effects of matrix stiffness on PpIX production will be discussed (13). Functional targeting refers to approaches that target the unique properties of tumor tissues and the TME including: 1) abnormal vasculature, 2) tumor hypoxia, and 3) increased acidity in tumors. Targeted delivery refers to strategies that involve the use of targeting moieties that facilitate the binding of PS to malignant cells through a molecular recognition process (14). These strategies leverage the overexpression of certain biomarkers on malignant cells that are less expressed on healthy cells to achieve specificity. This review offers a perspective on how these targeted PDT approaches provide opportunities to modulate the cellular and non-cellular components of the TME, with a focus on tumor mechanical properties and survival. The implications for therapy design, taking into consideration the role of mechanical stress in the TME, are discussed.

## THE TUMOR MICROENVIRONMENT AS A TARGET FOR CANCER TREATMENT

### Mechanical Stress in the Tumor Microenvironment

Cells respond to environmental changes by receiving and processing signals that originate in the extracellular space using structures and mechanical linkages among cell surface receptors, the cytoskeleton, and the nucleus (15, 16). Mechanical signals from the extracellular space are sensed by the cells through integrins and other focal adhesion proteins. These signals are transduced through the cytoskeleton and effector signaling cascades to elicit a biological response, and this conversion of mechanical signals to biological responses is termed ‘mechanotransduction’ (17). Many of the components of focal adhesion assembly are also involved in the cell migration process, and mechanical stress can induce migration (18). The tumor cell response to mechanical inputs can also be indirect, as mechanical stresses can influence transport, impeding drug delivery and altering oxygen tension and tumor acidity (19). Tumor cells can be exposed to a variety of mechanical inputs, including solid stress, interstitial fluid pressure (IFP), and flow-induced shear stress. Mechanical changes in the environment may promote tumor progression by activating oncogenic signaling pathways or by preventing therapeutics from reaching the target site.

**Solid stress.**—Solid stress is mechanical stress that arises from the solid components in tissue (as opposed to stresses arising from fluid pressures and flows), and changes in solid stress are due to changes in both the cellular and non-cellular components of the tumor. Cell-cell and cell-extracellular matrix (ECM) dynamics, in addition to the rapid accumulation of

mass due to cell proliferation and cell recruitment, induce deformation of local tissue and can increase tumor solid stress in a process termed the ‘mass effect’ (20, 21). Furthermore, tumor ECM, including stiff collagen fibrils and incompressible hyaluronic acid, can resist tumor growth, promote apoptosis in mechanically compressed cells (22–24), and contribute to solid stress propagation in tumors (25). While these effects may impede tumor growth, studies using single cells or 3D spheroids in confined spaces or under mechanically applied compression have revealed that increased compressive stress leads to increased invasiveness of cancer cells (26–30).

Tumors are inherently biphasic, consisting of a solid phase hydrated with interstitial fluid. Thus, compressive stresses, due, for example, to a tumor growing in a confined space, result in increased fluid and solid stress, but isolating the specific contributions of solid stress in a tumor is challenging. Nia and colleagues developed methods for isolating and measuring solid stress, specifically, by quantifying the deformation of resected tumors after dissection to release residual stresses (31). When tumors bearing large solid stresses are cut along a plane, solid stresses at the newly exposed surface are released and the tumor tissue deforms in a manner dependent on local stresses prior to the cut. Using this method, the authors measured solid stress in a xenograft brain tumor as 0.21 kPa and in a xenograft pancreatic ductal adenocarcinoma tumor as 7 kPa. In another recent study by Nieskoski and colleagues, a Millar pressure sensor and wick-in-needle technique were used in concert to measure total stress and IFP locally within a tumor (32). The solid stress was then defined as the total stress less the IFP, and a solid stress of 2.67 kPa was measured in a human pancreatic adenocarcinoma xenograft. Other studies have sought to study how solid stress is spatially distributed within tumors, revealing that while the core of the tumor is often under compressive solid stress, the periphery is often under tension, and this distribution of stress is supported by computational modeling. (20, 33–35).

Matrix stiffness signals to tumor cells independent of its contributions to solid stress, and the effects of matrix stiffness on tumor biology have been well-studied using 2D and 3D models. As noted above, cells are exquisitely sensitive to mechanical signals from the extracellular environment, and in cancer cells, the responses to matrix stiffness can have downstream impacts on migration, proliferation, survival and invasiveness (23, 36–43). Moreover, gradients in stiffness and the alignment of collagen fibers may influence directional cell migration by durotaxis and alignotaxis, respectively (44).

However, while compressive stress and a rigid extracellular environment can promote invasive behavior, it is important to recognize that stiffness of the ECM is intertwined with its biochemical composition, which in itself regulates growth and invasive behavior. For example, ECM (rich in collagen I) promotes invasive behavior in 3D tumor models, as compared to laminin-rich ECM, which inhibits invasiveness (45) (36). For these reasons, there have been a number of efforts to design experimental models which enable tuning of mechanical properties independently from matrix biochemistry (46–49). Collectively, the literature points to the complex interplay between matrix mechanical properties and biochemical composition, to both promote and constrain tumor invasiveness and proliferation, depending on the context. Outside of mechanical cues that activate invasive behavior initially, the degree of motility acquired is further regulated by both ECM

composition and cellular expression of matrix remodeling enzymes, such as matrix metalloproteinases (MMPs) (Figure 3) (50).

**Interstitial fluid pressure.**—Interstitial fluid, i.e. the fluid in the spaces between cells, is estimated to comprise 20% of the body's mass and is important for oxygen, nutrients, and waste exchange between the vascular system and cells (51). The IFP of a normal tissue is close to zero and there is a small negative pressure gradient between the interstitium and capillaries, resulting in an outward transcapillary flow. This small fluid flow from capillaries to the interstitium and on to lymphatics is mainly regulated by the hydrostatic and colloid osmotic pressures of capillaries and the interstitial space (52).

In pathological conditions such as cancer, interstitial fluid that infiltrates tumor tissue from leaky blood vessels and inflammation increases IFP (53). Additionally, inadequate or non-functional tumor lymphatic vessels (e.g. due to compressive stress) can lead to insufficient drainage, which, together with altered tumor transport environment, leads to a net pressure gradient between the tumor and surrounding tissue. Elevated IFP is observed in many solid tumors (34, 52, 54). For example, Curti and colleague measured the mean IFP of melanoma nodules from 22 patients as 29.8 mmHg (55). Another study by Nathanson and colleagues measured the mean tumor IFP from ductal carcinoma patients as 29 mmHg (56). In another pancreatic ductal adenocarcinoma xenograft study, Provenzano and colleagues showed that the tumor IFP ranged from 75–130 mmHg (57). An important implication of increased tumor IFP is potentially increased difficulty in delivering therapeutics. Additionally, Hofmann and colleagues showed that the stretching of cancer cells at the tumor cortex due to IFP triggers MAPK-associated cell proliferation (58). Increased fluid pressure in tumors may cause tumor progression and metastasis due to the leaking of growth factors and cancer cells from blood vessels that are located in the tumor boundary to the surrounding host tissue (21). Furthermore, the pressure gradient in the tumor margin, because of high tumor IFP, causes higher interstitial flow into the tumor stroma and the surrounding lymphatic vessels (59). The effects of altered transport caused by elevated interstitial flow on cancer cells have been studied extensively by using different microfluidic tools. Increased interstitial flow contributes to tumor progression by promoting the activation of fibroblasts (54, 58, 60). Shields and colleagues showed that interstitial flow causes autocrine secretion of CCR-7 ligands, and therefore CCR7-dependent migration along the flow direction in three breast cancer cell lines (61). The results of a relevant study from Polacheck and colleagues supported the same idea using another breast cancer cell line: MDA-MB 231. However, they revealed that there is another CCR7-independent, integrin-activated mechanism that derives migration in the opposite side of interstitial flow (62). Another study by Polacheck and colleagues showed that the same cancer cell line reacts to interstitial flow drag by reorganizing their focal adhesions. This adaptation balances the stress at the upstream side and causes migration on the upstream direction of interstitial flow (17). Macrophages are another cell type that migrates against the flow. Li and colleagues showed that interstitial fluid flow from the tumor to the surrounding tissue not only induces M2 polarization of macrophages, but also changes their migration direction towards the tumor masses, causing M2 macrophages to contribute more to tumor progression (63).

**Flow-induced shear stress.**—Tumors in intestines, stomach, or other parts in the peritoneal cavity are exposed to movements of body fluids, such as gut contents, gastric juice, and ascites (64). In contrast to the stress that is initiated by solid components and interstitial pressure, the stresses initiated by fluid flow over tissue and cells are shear stress and drag (19). Avvisato and colleagues, who were focusing on flow-induced shear stress on colon cancer cells, demonstrated that shear stress has contradictory effects on the proliferation rate of different colon cancer cell lines (64). Fluid ascites in the peritoneal cavity are normally cleared out by the host system, however in pathological conditions such as cancer, it may build up (65, 66). Accumulation of malignant ascites is accepted as a poor clinical outcome and one of the reasons for metastasis of ovarian cancer (65). To investigate the effects of fluidic forces in a 3D ovarian cancer model, Rizvi and colleagues used a microfluidics platform (66). Results of the study have shown that 3D ovarian cancer micronodules, grown under continuous laminar flow, exhibited an aggressive and invasive phenotype, including altered tumor morphology, upregulated EGFR expression/activation, and increased EMT.

### The tumor microenvironment

A solid tumor is not only made up of genetically disrupted proliferating cells, but also a dense and rich tumor stroma containing cellular and non-cellular components of healthy tissue, such as fibroblasts, immune cells, adipocytes, proteoglycans, hyaluronan and fibrous proteins (44). The dynamic milieu where complex heterotypic interactions between cancer cells and stroma take place is called the TME (67). Abnormal angiogenesis and activation of fibroblasts are key phases during tumor progression (68). Activated fibroblasts mediate the formation of a dense, collagenous ECM in solid tumors, which is called desmoplasia (69). Furthermore, there are chemical and physical gradients in tumor tissue, such as regions of hypoxia, differences in pH, and other chemical gradients. Desmoplasia, hypoxia, and other stromal components may synergize with tumor progression and mitigate treatment success (44).

**Stromal components.**—The stroma provides structure to the tissue or organ that contains many cell types in order to maintain homeostasis (70). When cancer develops in tissue, cancerous cells come into close contact with the stroma, and genetic alterations in tumor cells change the stromal components, leading to an environment that contributes to cancer proliferation. During early cancer development, the basement membrane degrades, allowing activated stroma to come into direct contact with cancer cells (70), (71). Tumor stroma can consist of fibroblasts, immune cells, ECM components, and other tissue-specific cells, such as adipocytes. Additionally, endothelial cells and pericytes form the tumor vasculature. The accumulation of endothelial cells, fibroblasts, and immune cells within a tumor is governed by growth factors that are released by cancer and cancer-associated cells. The interactions between tumor cells and stromal cells, via soluble factors or cell-cell interactions, may cause functional changes that support tumor growth (67, 72). For example, tumor endothelial cells can become more proliferative, and quiescent fibroblasts can become activated. Another contribution of tumor endothelial cells and cancer-associated fibroblasts (CAFs) to tumor survival is mutual energy production. The metabolic heterogeneity between stromal cells and cancer cells supports the survival of cancer cells by buffering and recycling the products

of their anaerobic metabolism (73). Tumor associated macrophages (TAMs) are another type of stromal cell that is often present in the TME. Macrophages are a first line of defense against pathogens. Classically activated macrophages, which are also known as M1-polarized macrophages, can kill cancer cells. However, one of the two subgroups of macrophages, M2-polarized (a.k.a. alternatively activated macrophages) are strongly associated with cancer progression (74). Research has shown that M2 macrophages contribute to tumor progression and suppression of antitumor immunity by expressing cytokines and chemokines (75).

CAFs are considered distinct from fibroblasts that are found in normal tissue, but the sources of CAFs remains unclear (76). According to some studies, CAFs are differentiated from endothelial cells by endothelial-mesenchymal transition (68). Other theories suggest that normal fibroblasts, which are quiescent single cells located in the interstitial space, are activated by certain growth factors, such as EGF and transforming growth factor- $\beta$  (TGF- $\beta$ ), a cytokine that also plays important role in tumor progression and EMT (77, 78). An activated fibroblast is characterized by the expression of alpha-smooth muscle actin ( $\alpha$ -SMA) and shows more migratory capacity (67). Furthermore, CAFs secrete increased levels of chemokines and growth factors, which contribute to tumor progression and therapeutic resistance (79). Research has shown that CAFs play an important role in TGF- $\beta$  signaling, which regulates epithelial-mesenchymal transition (78, 80, 81). Additionally, matrix metalloproteinase-3 (MMP-3), a product of CAFs, promotes EMT by initiating the cleavage of E-cadherin. CAFs also affect dendritic cell function and inhibit cytotoxic T cell recruitment and survival that is mediated by TGF- $\beta$  secretion (82). The CAF- derived release of vascular endothelial growth factor (VEGF) also affects dendritic cell generation and maturation by reducing MHC class II expression and the ability to internalize antigens (83, 84). Lastly, CAFs can remodel the ECM by secreting ECM-degrading proteases, such as MMPs (67).

The ECM is a porous and biphasic material that surrounds the space between cells. By forming fibrils and sheet-like structures, the ECM provides structural integrity and mechanical support to the tissue (51), (85). The mechanical properties of the ECM, in part, determine the mechanical properties of the tissue (17). The main constituents of the ECM are water, proteoglycans and fibrous proteins such as collagen and elastin (86). The hypoxic and heterogeneous TME with increased inflammation results in remodeling of the ECM. This process, where inflammation occurs and the density and stiffness of ECM increases, is similar to wound healing, which is why cancer is often described as a wound that does not heal (87, 88). Additionally, the contribution of activated fibroblasts is similar in the wound-healing process and cancer, leading to a buildup of ECM components, such as hyaluronic acid and collagen (67, 89). The increase in density and stiffness of the ECM in cancer plays a vital role in tumor progression. Critical biomechanical and biochemical cues that regulate adhesion, migration, differentiation, and proliferation are, in part, provided by the tumor ECM (90, 91). Furthermore, collagen fibrils of tumor ECM may align in a way that influences metastasis or the form of migration tracks (86).

In considering the influence of ECM components on interactions in the TME, it is important to consider not only the composition of the ECM itself but also the mechanisms by which

cells interact with the ECM. For example, integrins are a family of proteins that form transmembrane heterodimers, and play a vital role in transducing mechanical signals from ECM components such as fibronectin, collagen, laminin, and vitronectin by providing a linkage to the internal cytoskeleton (92). Given the complex role of integrin-mediated signaling in regulating tumor growth and progression, it is not surprising that some integrins have emerged as therapeutic targets in cancer (93, 94). For example, fibronectin (FN) is assembled by CAFs and triggers cancer cell invasion, mostly via integrin  $\alpha_v\beta_3$  (95). Integrin  $\alpha_v\beta_3$ , which is considered a marker for breast, lung, and pancreatic carcinomas, is also associated with drug resistance (96).  $\alpha_5\beta_1$  is another integrin that has been reported to have a pro-migratory effects resulting from FN alignment by CAFs (97). In this review, we will highlight studies that investigate the impact of PDT on the ECM as well as integrin heterodimers that mediate mechanical interaction with ECM components and may form the basis for targeting strategies.

**Hypoxia and acidosis.**—Hypoxia is common in most solid tumors and is a negative prognostic indicator because of its contribution to angiogenesis, chemoresistance, and metastasis (98). As reviewed by Muz and colleagues, the oxygen concentration in tumors can decrease up to 96%, relative to comparable normal tissue (99). For example, oxygen percentage has been shown to drop from 8.5% to 1.5% in normal breast tissue versus cancerous breast tissue. Similarly, median oxygen percentages are 7.5% and 0.3% in normal pancreas tissue and pancreatic tumor, respectively. One of the main causes of tumor hypoxia is the rapid proliferation of cancer cells, which increases both the rate of oxygen consumption and the distance between blood vessels and cells (100, 101). As discussed elsewhere in this review, solid stress also causes increased hypoxia due to its compressive effects on the blood and lymphatic vessels inside a tumor. Narrowing of blood and lymph vessels leads to decreased oxygen and nutrient levels in tumor tissue, resulting in hypoxia and a decrease in pH in the TME (21, 22, 31). Furthermore, this hinders the delivery of therapeutics and facilitates the escape of cancer cells from the site of the primary tumor by increasing IFP (19). Multiple intracellular signaling pathways are triggered by hypoxia. The family of translational regulators, HIF (hypoxia-inducible factor), mediates the adaptation of cells to the hypoxic microenvironment. The accumulation and activation of HIF results in the transcriptional activation of certain genes that are involved in cell survival, angiogenesis, and invasion (102). HIF-1 also mediates a metabolic shift in cancer cells, whereby cancer cells switch from oxidative phosphorylation (aerobic) to glycolysis (anaerobic). The byproducts of anaerobic metabolism cause acidosis in the TME. Furthermore, this harsh hypoxic and acidic microenvironment creates a survival advantage for aggressive cancer cells (21). Other intracellular signaling pathways stimulated by hypoxia are PI3K/AKT and MAPK, which are associated with cell proliferation and survival (99). Furthermore, tumor hypoxia is associated with the increased secretion of TGF- $\beta$  and VEGF, and the suppression of immune response (24). Additionally, hypoxia leads to metastasis by increasing TGF- $\beta$  and proteins that are involved in EMT (103).

**The enhanced permeability and retention effect.**—The enhanced permeability and retention (EPR) effect is a feature of the TME that is characterized by abnormally high leakage of blood plasma components from the tumor vasculature, as well as their increased

retention in tumors (104). Enhanced vessel wall permeability arises from the unique physiology of the tumor vasculature. Normal vasculature in healthy tissues is hierarchically organized, enabling the efficient delivery of oxygen and nutrients (105). Tumor vasculature, on the other hand, is disorganized, tortuous, and hyperpermeable. The development of this vasculature occurs through aggressive cancer cell growth and overexpression of pro-angiogenic factors to accommodate their high metabolic needs (53, 104, 105). Tumor vessels are also immature, lacking a normal basement membrane, smooth muscle cells, and pericytes. Immature vessels, in combination with the presence of large fenestrations, cause hyperpermeability of the tumor vasculature to macromolecules and nanoparticles (52, 105–107). This enhanced extravasation is accompanied by poor lymphatic clearance, leading to the enhanced retention of extravasated particles (104, 106). The vasculature in most nonpathological tissues is less permeable than tumor vasculature, attenuating drug accumulation in healthy tissues (108). Therefore, the hyperpermeability of tumor vasculature and insufficient lymphatic drainage in tumors, in contrast to normal tissues, drive the EPR effect, which has been exploited for the selective delivery of anticancer drugs to tumor tissues (107).

The EPR effect is closely related to high IFP in tumors. The immature, hyperpermeable vasculature allows for extravasation of plasma fluid and proteins into the interstitial space, and the lack of lymphatic drainage prevents clearance, causing the fluid to accumulate (108, 109). Additionally, as the tumor grows, it compresses lymphatic vessels, further decreasing drainage of interstitial fluid (108, 110). As a result, while the IFP in normal tissue is around zero or slightly negative, tumor IFP is significantly higher and can reach above 90 mmHg (111). High IFP at the tumor site hinders the EPR effect through decreasing the pressure gradient in the interstitial space, thereby limiting the convective flow that is normally the dominant mechanism of transport in tissue for macromolecules and nanoparticles (110, 112). Therefore, a consequence of high IFP is heterogeneity in the extent of the EPR effect, limiting nanoparticle drug delivery and causing differences in therapeutic outcomes between patients. This relationship was confirmed in a mathematical model developed by Jaffray *et al.* (113) that associated liposome accumulation to the transport properties of solid tumors. They found that variations in peak IFP can cause inter-patient heterogeneity in liposome accumulation. To address the influence of abnormal vasculature on tumor IFP, anti-angiogenic therapies have been developed to normalize tumor vasculature (114). According to a model by Jain *et al.* (115), such antiangiogenic therapies can modulate the TME through increasing intratumoral convection and decreasing fluid convection into the peritumor tissue or fluid. Increasing intratumor convection improves drug penetration and distribution, while decreasing fluid convection out of the tumor decreases the likelihood of lymphatic metastasis, peritumor edema, and ascites formation.

## TARGETING THE TUMOR MICROENVIRONMENT WITH PHOTOCHEMISTRY

There is a breadth of research investigating how chemotherapeutics, biological agents, and radiotherapy can be leveraged to target the TME through preventing neovascularization, overcoming hypoxia and inhibiting the contribution of stromal cells to tumor progression (101, 116, 117). PDT is a minimally-invasive treatment modality that is used for oncologic and non-oncologic applications, and has been explored for the modulation of the TME (118–

120). The cytotoxic mechanism of PDT is based on inducing photodamage through the excitation of a non-toxic photoactive chemical, a PS, using light of a specific wavelength (121). A PS, in singlet ground state, absorbs a visible photon of appropriate energy, and becomes electronically excited to a singlet excited state. The PS then either decays to the singlet ground state by generating fluorescence or undergoes intersystem crossing to the triplet excited state. From there, the molecule can interact directly with molecular oxygen or with another substrate via electron or proton transfer to return to the singlet ground state. When these photochemical reactions result in the generation of sufficient amounts of singlet oxygen or other reactive molecular species to cross the threshold of cell survival, toxicity is conferred to the target tissue, such as cancer cells (121, 122).

The modes of cell death activated by PDT (e.g. apoptosis, necrosis, necroptosis, lethal autophagy, or paraptosis) depend strongly on the type of PS used and the sub-cellular and/or extracellular PS localization at the time of light activation. Mitochondrial photodamage generally leads to the initiation of apoptosis through the direct release of cytochrome c and degradation of the anti-apoptotic Bcl family of proteins, without effects on pro-apoptotic Bax (5, 123, 124). The initiation of apoptosis by direct mitochondrial photodamage is significant in cancer therapy because this pathway bypasses many of the escape and repair mechanisms through which cancer cells are able to develop resistance to traditional treatments. PDT can also cause toxicity by initiating necrosis, and causing white blood cells to release cytokines, such as necrosis factors (125, 126). Depending on the type of photodamage and the underlying biology of the target cells, PDT can also cause lethal levels of autophagy (127), or as has been reported more recently, can trigger paraptosis, a response, in part, to misfolded ER proteins (128). Combining PS or PS formulations to enhance PDT- efficacy by targeting complementary tumor compartments or sub-cellular sites, has also shown promise (129–136). Importantly, because the timing, location, and intensity of light activation can be carefully controlled, PDT is inherently a targeted therapeutic modality. Exploitation of PDT-mediated cytotoxic mechanisms has been used in combination with conventional and emerging therapies to overcome chemoresistance (137) and to enhance efficacy (138–143).

In addition to inducing spatially and temporally selective cytotoxicity, PDT can also alter the TME by targeting specific malignant and non-malignant cells as well as extracellular components. This damage is highly dependent on PS localization, which is dictated by the structural and chemical properties of the PS and the drug light interval (the time interval between drug administration and light exposure). Some PSs localize preferentially in specific tumor compartments, such as Tookad, which largely stays in the vasculature (144), (145). Other PSs, such as benzoporphyrin derivative (BPD), can target various tumor compartments (e.g., vasculature, ECM, cancer cells) depending, in part, on the PS-light interval. The use of Tookad and BPD in the context of vascular-targeted PDT is further discussed in a later section. The localization of the PS directly influences the treatment outcome. For PDT targeted to the vasculature, there can be a range of effects, including vascular permeabilization for the enhanced delivery of nanoscale therapeutics, as well as blood vessel occlusion which can result in increased tumor hypoxia (146–149). Additionally, PDT that is targeted to the ECM can alter ECM composition through hyaluronic acid degradation and collagen crosslinking (150–152). PDT-induced collagen crosslinking is

being researched for the treatment of Keratoconus of the cornea and intimal hyperplasia mediated vascular cell migration (153, 154). However, PDT can also lead to the degradation of collagen through damaging fibroblasts and causing the release of MMPs (155), (156). While the degradation of collagen prevents desmoplasia and increases drug penetration, it may also lead to increased invasion and metastasis of cancer cells (Figure 4) (91, 157), (158). Therefore, the effects of PDT on ECM composition can be highly varied, and destruction of stromal components does not necessarily improve treatment outcomes. For example, previous work has shown that the depletion of the heterogeneous stroma results in more aggressive cancer behavior. In one study, a transgenic mouse was generated with the ability to delete  $\alpha$ SMA<sup>+</sup> myofibroblasts in pancreatic cancer, and the depletion of the stroma caused invasive tumors with diminishing mouse survival (159). Therefore, destruction of stromal components could aggravate disease progression, so PDT treatments designed to target stromal components must be carefully studied and optimized. A summary of PSs that are commonly used in clinics and in preclinical research is presented in Table 1, along with their localization characteristics (132, 160–170).

Spatiotemporal targeting is inherent to PDT, based on PS localization properties, PS-light interval and spatial confinement of light-based activation. Targeted PDT can also be achieved by conditioning the target cells prior to PDT in order to improve the intracellular accumulation of the PS. This strategy has primarily been implemented for the targeting of PpIX. The specific delivery of PSs to particular tissues and cell types can also occur through incorporating monoclonal antibodies, nanoparticles, and targeting moieties into PDT treatment strategies. This review categorizes approaches for achieving targeted PDT into three central areas: I.) targeting by cellular and tissue modulation, II.) functional targeting, and III.) targeted delivery. Targeting by cellular and tissue modulation refers to methods that strategically alter biological processes to improve PDT treatment efficacy. Functional targeting encompasses approaches that leverage the unique properties of the TME, such as abnormal vasculature as well as tumor hypoxia and acidity, to achieve selectivity. The third strategy, targeted delivery, involves approaches that use drug and PS carriers, and targeting moieties, for selective tumor destruction. This chapter discusses these various methods for targeting PDT to different components of the TME, as well as the effects of photochemistry on the mechanical and stromal interactions in tumors.

### Targeting by Cellular and Tissue Modulation

Cellular and tissue modulation is among the most translationally-relevant approaches to enhance selective treatment of target tissue. In the case of targeted PDT for cancer, a major goal of this targeting strategy is to increase the accumulation of PSs in tumors. Cellular and tissue modulation, also known as biomodulation, is the alteration of biological mechanisms by which cells metabolize, take up, or retain PSs to selectively enhance PDT efficacy (12). A focus of this section of the review is the heme biosynthesis pathway utilized in mammalian cells, also known as the Shemin pathway, which involves the conversion of 5-ALA to heme (171–177). The penultimate step in this pathway is the production of PpIX (Figure 5a). A preferential site of localization of PpIX is the mitochondria (169). PpIX can also be transported into the cytosol by mitochondrial ATP-binding cassette transporter G2 (ABCG2) (178, 179). The production of PpIX can be increased by modulating key enzymes in the

heme pathway, such as coproporphyrinogen (CPO) and ferrochelatase (FECH), as summarized in Table 2. ALA is a prodrug that is approved by the FDA for fluorescence-guided resection of gliomas and photodynamic treatment of actinic keratosis (180–183).

Preferential accumulation of PpIX in cancer cells results from dysfunctional activity of key enzymes in the heme pathway compared to healthy tissue. This includes decreased FECH activity and increased CPO activity, which increases the production of PpIX and limits its conversion to heme, leading to increased accumulation of the PS in target tissue (184). In 1979, Malik and Djaldetti first showed that ALA enhanced the synthesis of hemoglobin as well as the intermediate precursor uroporphyrin and PpIX (185). Later, in 1987, eighty basal cell carcinomas (BCC) were treated using ALA-induced PpIX-based PDT by Kennedy and Pottier, with a 90% response rate (186–188). Among the advantages of PpIX is that it is rapidly cleared from the skin from topical, systemic, oral, or intradermal administration, thereby minimizing skin phototoxicity (189, 190). Difficulties arise in using this treatment due to insufficient or non-uniform PpIX accumulation in the cancerous tissue, highlighting the need for approaches such as cellular and tissue modulation.

To overcome the problem of insufficient or non-uniform PpIX accumulation, various methods to modulate the heme pathway have been developed. Cells that are poorly differentiated and rapidly proliferating, as is common in many tumors, may produce insufficient amounts of PpIX (12). One area of investigation to address this issue involves the use of cellular differentiators such as vitamin D or its analogues, methotrexate, retinoic acid, 5-fluorouracil acid, iron chelators, and the androgens 5 $\alpha$ -dihydrotestosterone (DHT) and R1881 (191–217).

Treatment efficacy can be influenced by microenvironmental factors such as temperature, pH, and oxygen availability/hypoxia (218–223). An emerging area of investigation is the role of mechanical stress on PpIX production and accumulation. A study by Niu *et al.* (13) using two glioma cell lines of bulk/solid tumors, U373 and U118, showed that cell proliferation rate increased in a nonlinear fashion as substrate stiffness increased. Their motivation was to study cell proliferation and PpIX synthesis in glioma cells on substrates simulated the tissue stiffnesses of normal brain (1 kPa) and glioblastoma (12kPa) (13, 224, 225). The two cells used to evaluate the effects of mechanical stiffness were selected based on a previous study of PpIX production in a panel of 10 glioma cell lines. U373 was determined to produce the most PpIX, while U118 produced the least (226). Evaluation of PpIX production in these two cell lines on substrates of varying stiffnesses showed that the mechanical properties of the underlying matrix affected each cell line differently. In the U118 cell line, a stiffer microenvironment led to increased PpIX accumulation with no change in the rate of cell growth (13). In contrast, substrate stiffness had no significant effect on PpIX accumulation in the U373 cell line (Figure 5b) (13). In another study by Ulrich *et al.*, micromechanical cues from the ECM on glioma cells was evaluated by testing various ECM substrates with different mechanical and biochemical properties. It was found that ECM elasticity strongly affects glioma cell structure, motility, and proliferation (224). These findings highlight the impact of the ECM on cell morphology, cytoskeletal organization, motility, and control of MMII-mediated intracellular contractility (224). Further studies must

be done to clarify the effects of mechanical stiffness on PpIX production in glioma and other cell types.

### Functional targeting

The TME acquires a unique set of biochemical traits which are closely connected to tumorigenesis (227). While this distinct TME is linked to proliferation and metastasis, it also provides opportunities for the development of PSs that target these unique features through a strategy termed *functional targeting*. One aspect of functional targeting is the EPR effect, which causes an increase in nanoparticle accumulation and retention at the site of a tumor due to hyperpermeable tumor vasculature and insufficient lymphatic drainage. This phenomenon has been exploited for cancer treatment through the design of nanomedicines for drug targeting to tumors, though there is significant heterogeneity that limits the influence of the EPR effect on drug localization (109, 228, 229). Various photochemistry-based strategies have been employed to enhance the EPR effect through vascular permeabilization to improve nanomedicine extravasation in tumors. PDT has also been used clinically to occlude vasculature, with the goal of restricting the supply of blood to the tumor. Other unique features of the TME that are leveraged to achieve *functional targeting* include hypoxic and acidic conditions (Figure 6). As discussed in a previous section, tumors develop hypoxic conditions due to an imbalance in oxygen supply and consumption (100). The abnormal, disorganized vascular network that develops in the TME provides limited oxygen supply despite an increasing demand for oxygen generated by the rapidly growing tumor. One of the byproducts of the hypoxic microenvironment is the development of acidic conditions (230). In the absence of oxygen, cancer cells use anaerobic glycolysis, leading to lactic acid production and a decrease in pH (231). Interestingly, even when oxygen is abundant and mitochondria are fully functional, cancer cells can utilize aerobic glycolysis, producing lactate despite the availability of oxygen. This is termed the Warburg Effect, first described in the 1920s by Otto Warburg (232). This section will discuss functional targeting, through which the unique features of the TME, such as abnormal vasculature, acidity, and hypoxia, can be leveraged to achieve targeted PDT.

**Exploiting the enhanced permeability and retention effect and targeting the tumor vasculature.**—The EPR effect, first discovered by Matsumura *et al.* (233), allows nanoscale drugs to passively accumulate preferentially at the site of a tumor. While many nanomedicine formulations claim to leverage the EPR effect for specific delivery to cancer cells, there has been recent discussion regarding critical limitations to the EPR effect and the models used to study it that hamper its true influence on nanoparticle accumulation (234). PDT has demonstrated potential as a strategy to address limitations in the EPR effect and increase nanoparticle extravasation at the tumor site.

As discussed in a previous section, the EPR effect occurs due to the tendency of tumors to develop abnormal vascular networks with poor lymphatic drainage. An imbalance of pro-angiogenic and anti-angiogenic signals at the tumor site leads to the development of abnormal vascular networks, which often lack the organization of typical vascular networks, and are tortuous and dilated (53). This vascular network often exhibits large pores, enabling increased extravasation of nanoparticle drug carriers into the tumor site for heightened drug

accumulation. Vasculature in nonmalignant tissue has smaller fenestrations, thereby limiting drug accumulation in healthy tissues and minimizing adverse side effects (108). The high extravasation in tumor vasculature is accompanied by poor lymphatic drainage, leading to increased drug retention (235).

Knowledge of the EPR effect has had widespread effects on the development of drug delivery systems for cancer, and various PS delivery vehicles have been developed that leverage the EPR effect to increase intra-tumoral PS accumulation (236). Examples of nanoparticle delivery vehicles that have been employed for PS delivery include liposomes (237–241), quantum dots (242, 243), viruses (244, 245), virus-like particles (VLPs) (246, 247), polymeric nanoparticles (248), silica nanoparticles (249, 250), metal nanoparticles (251), carbon nanoparticles (252, 253), and others (254–256). While the EPR effect has been used as the foundation for the development of a myriad of nanoparticle drug delivery systems, it has shown limitations in clinical practice due to high heterogeneity (109). Due to this heterogeneity, predictive nanotechnology is being developed to determine if a tumor is likely to accumulate nanoparticle drugs through EPR (257). For example, ferumoxytol (FMX), a 30 nm magnetic nanoparticle, when administered intravenously and visualized with magnetic resonance imaging (MRI), was shown to predict both the intratumoral accumulation of therapeutic nanoparticles, as well as their anti-tumor effect (258, 259). Such technology could be used to stratify patients based on EPR effect, and therefore has significant implications for personalized medicine in oncology.

The heterogeneity of the EPR effect occurs due to a variety of parameters that can differ widely between tumors, such as vascular maturation, tumor cell density, type of cancer, and IFP, among many others (109, 260, 261). Additionally, there are key limitations in how the EPR effect is studied. For example, it has primarily been evaluated in implanted tumors rather than metastatic tumors, despite the fact that metastases account for 90% of cancer deaths (234, 262). Additionally, the EPR effect is primarily studied in animal models that poorly recapitulate human tumors (263). Due to heterogeneity in the extent of the EPR effect, methods to improve permeability of tumor vasculature are of great interest for improving drug delivery and therapeutic outcomes. PDT has been utilized as a novel method to achieve this. For example, through understanding pharmacokinetics following PS administration, drug-light interval can be optimized to activate PSs while they are accumulated in specific compartments to increase permeability to macromolecules and nanoparticles (8, 140, 143, 264, 265). Moreover, targeting moieties can be utilized to achieve accumulation of PSs in the tumor vasculature and perivascular tumor cells to enhance the EPR effect (266–268).

A study by Snyder *et al.* (147) explored the ability of low-irradiance PDT to permeabilize vessels to macromolecular agents, including fluorescent microspheres and liposomal doxorubicin (Doxil). Using a murine colon cancer model, when fluorescent microspheres were administered immediately following PDT, there was an increase in intratumoral accumulation of microspheres in the range of 0.1 to 2  $\mu\text{m}$ . When using low fluence rate PDT prior to Doxil administration, there was a significant increase in Doxil content in tumors, as well as up to 80% long-term tumor control. Additionally, a study by Gil *et al.* (148) used PDT as a method to improve the delivery and efficacy of oncolytic vaccinia virus (OVV) to

primary and metastatic tumors in mice. Tumors that received PDT treatment ( $128 \text{ J cm}^{-2}$  at  $14 \text{ mW cm}^{-2}$ ) 12 hours prior to OVV administration had an over 10-fold increase in viral titres compared to the control tumors. However, PDT with other light doses ( $135 \text{ J cm}^{-2}$  at  $75 \text{ mW cm}^{-2}$  and  $48 \text{ J cm}^{-2}$  at  $7 \text{ mW cm}^{-2}$ ) was less effective, underscoring the importance of treatment optimization when using PDT to increase intratumoral accumulation of therapeutics.

While PDT alone can be used to permeabilize tumor vasculature, targeting moieties can be incorporated to increase binding affinity to target cells. For example, Zhen *et al.* (267) synthesized PS-encapsulated ferritin nanocages with peptides targeted to  $\alpha v \beta_3$ , an integrin that is overexpressed in neoplastic endothelial cells. When used prior to nanoparticle administration, these endothelium-targeted PSs caused an increase in nanoparticle accumulation in tumor tissues by  $\sim 20$ -fold. When targeted PDT was used prior to treatment with the anti-cancer drug Doxil in a xenograft breast cancer tumor model, an increase in treatment efficacy of 75.3% was observed. SEM images confirmed that the increased nanoparticle accumulation could be attributed to large fenestrae in the endothelial walls. Additionally, Sano *et al.* (268) showed that photoimmunotherapy (PIT) can be used to achieve an increase in the EPR effect, termed the super-enhanced permeability and retention (SUPR) effect. Following the light activation of panitumumab-IR700 constructs that accumulated in perivascular tumor cells, they observed significantly higher extravasation of a variety of nanoscale particles. This is attributed to the ability of PIT to cause necrosis specifically in the antigen-expressing cancer cells in the perivascular space while leaving nearby normal cells unharmed (269).

Previous work has also demonstrated that PDT can cause time-dependent changes in tumor IFP, which is normally a barrier to EPR-mediated drug accumulation in tumors (110, 112, 270). A study by Leunig *et al.* (270) showed that PDT caused an initial increase in tumor IFP immediately following light administration, but 24 hours after PDT, tumor IFP dropped to 50% of the control in a hamster melanoma model. In another study, Perentes *et al.* (149) investigated the IFP alterations caused by PDT as well as the resulting changes in the accumulation of liposomal doxorubicin. The authors showed that low-dose photodynamic therapy (L-PDT) reduces tumor IFP without impacting normal tissue IFP. Additionally, when liposomal doxorubicin was administered following L-PDT treatment, the drug penetrated significantly deeper into the tumor tissue compared to the control. Recently, Cavin *et al.* (271) explored the mechanism through which L-PDT alters vasculature to modulate IFP. Using a pericyte and endothelial cell coculture, they found that PDT alters the function of pericytes, strengthening their association with endothelial cells. Tumor vasculature typically has poor pericyte coverage (52), so increasing pericyte-endothelial cell association causes vascular normalization, leading to a decrease in IFP and an increase in convective transport of drugs into the tumor. These studies illustrate that PDT can have significant effects on tumor IFP, though the effects are dependent on many factors, including PS-light interval, light dose, and PS dose.

In addition to permeabilizing the vasculature to improve drug accumulation, vascular-targeted PDT has also been used to cut off blood supply to the tumor (272–275). WST-09 (Tookad, palladium bacteriopheophorbide) and WST-11 (Tookad soluble, Padeliporfin) are

PS with limited extravasation from vasculature, enabling spatially selective photodamage by confining PDT-mediated toxicity to the vascular compartment. When activated by light, Tookad can cause vascular occlusion, resulting in tumor necrosis (276–279). Clinical trials have confirmed that PDT using Tookad is a well-tolerated and effective approach for the treatment of prostate cancer (280–282). In one clinical trial, 28% of patients who received vascular-targeted PDT experienced disease progression after 24 months, compared to 58% of patients who underwent active surveillance (281). An extended follow-up study analyzed the same cohort and found that, at four years, patients who had received vascular PDT experienced significantly lower disease progression rates and were less likely to convert to radiotherapy (24% versus 53%) (282).

A primary, nononcologic, application of PDT for vascular occlusion is in the treatment of age-related macular degeneration (AMD), the leading cause of blindness in elderly adults in western countries (283, 284). The neovascular form of AMD (also known as exudative or “wet”) leads to the formation of aberrant blood vessels from the choriocapillaris under the foveal avascular zone below the retina (subfoveal choroidal neovascularization, CNV). These leaky blood vessels can cause loss of vision through subretinal hemorrhage and detachment of the retinal pigment epithelium (283). Although thermal photocoagulation has been used as a primary treatment method for destroying CNVs, this treatment method has drawbacks, including retinal scar formation and immediate loss of visual acuity (284, 285). Preclinical and clinical studies demonstrated that CNV occlusion and improvements in visual acuity were achieved by activating intravenously administered BPD with non-thermal laser irradiation at short PS-light intervals (while the PS is in the vasculature) (161, 286–289) to cause thrombosis of vessels and selective damage to endothelial cells (285). Vascular-targeted PDT with a liposomal formulation of BPD, Visudyne, is approved worldwide for the treatment of wet AMD and has been used in millions of patients. PDT can therefore have multiple effects on the vasculature, including permeabilization and occlusion, depending on treatment parameters. This underscores the necessity for carefully optimizing vascular targeted PDT treatment regimens to achieve specific, desired effects.

While PDT has great potential in the clinic to induce cytotoxicity in cancer cells, it has also emerged as a promising modality to improve the extravasation of nano- and micro-scale agents at the tumor site. This has been achieved either through targeting the vasculature directly, or through targeting the cells in the perivascular space. Additionally, localization of PS in specific regions, such as vasculature or perivascular cancer cells, can be achieved through the use of targeting moieties as well as through the optimization of drug-light interval. While preclinical studies are promising, there is more work that must be done to bring this treatment strategy from benchtop to bedside. For example, light delivery methods can be further engineered to ensure that light is delivered uniformly to maximize access to target tissues. Additionally, the parameters for PDT treatment must be further optimized to improve drug delivery. For example, varying PS concentration and the amount of light delivered to the vasculature could potentially change the size and number of fenestrations created in the endothelial walls. Optimizing these parameters is critical because nanomedicines vary in size. Similarly, the optimal time after PDT to administer nano- and micro-scale therapeutics could differ based on particle size, so more work should be done to characterize this thoroughly. Moreover, combinational treatment regimens that pair

carefully optimized EPR-enhancing PDT with nanoscale therapeutics still need to be evaluated in clinical trials to determine if this strategy can successfully overcome the heterogeneous EPR that often limits nanomedicine efficacy. Overall, due to the potential of PDT as an adjuvant to nanoscale cancer drugs, the development of these technologies could have extremely widespread implications for cancer therapeutics.

**Targeting the hypoxic microenvironment.**—Another feature that can be exploited for PS targeting is the hypoxic TME. Piao *et al.* (290) developed a PS that can only be activated under hypoxic conditions, such as those in solid tumors. They conjugated an azo moiety to a seleno-rosamine dye, blocking intersystem crossing and therefore blocking singlet oxygen generation. Under low oxygenated conditions, the moiety is cleaved from the dye, allowing singlet oxygen generation upon light activation. The drug, therefore, has increased specificity for the hypoxic TME, where it can be light-activated.

Additionally, PDT can induce hypoxia in tumor tissues through both reducing vascular perfusion and consuming oxygen (146). One study by Busch *et al.* (291) investigated how two different fluence rates, 38 mW/cm<sup>2</sup> and 75 mW/cm<sup>2</sup>, differentially impacted Photofrin-PDT-mediated oxygen depletion. They found that in tumors treated with 75 mW/cm<sup>2</sup>, there was significant hypoxia, even tissues in close proximity to the blood supply (vascular-adjacent tissues). Alternatively, in tumors treated with 38 mW/cm<sup>2</sup>, there was an insignificant increase in hypoxia in vascular-adjacent tissues. The oxygen consumption associated with PDT presents an issue for repeated PDT treatments, where decreasing oxygen levels in the tissues might diminish the efficacy of subsequent treatments. While this oxygen consumption can exacerbate hypoxia-associated proliferation and metastasis, some groups have taken advantage of this by developing treatments that incorporate both PSs and hypoxia-activated prodrugs for a synergistic effect. For example, Feng *et al.* (292) developed a liposome containing chlorin-6 in the hydrophobic bilayer and AQ4N in the core. Chlorin-6 is a second-generation PS that is activated by 660 nm light, and AQ4N is a hypoxia-activated prodrug. In hypoxic conditions, nontoxic AQ4N is reduced first to AQ4M, then to AQ4, which intercalates DNA to inhibit topoisomerase II (293). They found that following irradiation of the liposome, chlorin-6 is activated, inducing severe hypoxia. These hypoxic conditions catalyzed the activation of AQ4N, leading to significantly decreased tumor volume in a mouse model.

Similarly, Liu *et al.* (294) used upconversion nanoparticles (UCNPs) to encapsulate both a PS, silicon phthalocyanine dihydroxide (SPCD), and a bioreductive prodrug, tirapazamine (TPZ). Tirapazamine generates cytotoxic free radicals, which in aerobic conditions are oxidized back into the harmless parent compound. However, under hypoxic conditions, TPZ becomes highly reactive and causes strand breaks in DNA (295). Liu *et al.* (294) found that under normal physiological oxygenation conditions, TPZ had little cytotoxicity, but following PDT-induced hypoxia, TPZ toxicity increased significantly. These studies illustrate that PSs can be functionally targeted to the hypoxic TME conditions, inducing specific toxicity.

Moreover, there are many studies that show that the therapeutic effect of PDT can improve when combined with methods for decreasing hypoxia (296, 297). Some methods focus on

increasing the oxygen concentration by using oxygen carriers such as artificial red blood cells that contain PSs (298–300). Mild heating also improves the intertumoral blood flow in PDT. The process is called photothermal therapy (PTT) in which the rapid increase in temperature above the threshold value of 42–45 degrees Celsius can kill cancer cells (301). Performing fractional PDT treatment can also minimize the dependence on oxygen by allowing time for the replenishment of tissue oxygen (302).

**Targeting the acidic microenvironment.**—The low pH of tumors has also been exploited in the development of functionally targeted PSs. For example, Luo *et al.* (303) developed a self-transformable pH-driven membrane anchoring photosensitizer (pHMAPS) for acidic selectivity. The pHMAPS incorporates pH low insertion peptide (pHLIP), which adopts a random coil configuration in neutral physiological pH (~7.4), but changes conformation in a more acidic pH to an  $\alpha$ -helix structure. This conformational change induces insertion into the cell membrane for selective delivery of the PS to cells in acidic environments such as the TME (303), (304). In an *in vivo* biodistribution analysis, pHMAPS localization was compared to a peptide without the ability to change conformation, nonmembrane anchoring photosensitizer (NMAPS). They found a significantly higher accumulation of the pHMAPS in the tumor compared to NMAPS, demonstrating successful targeting of the acidic TME.

Another study that leveraged the unique properties of pHLIP was done by Yu *et al.* (305), in which pH-responsive hollow gold nanoparticles loaded with PSs were synthesized to target the acidic microenvironment. In this study, pHLIP was conjugated to the nanoparticle surface for selective delivery to cells at low pH. Upon light activation, the nanoparticles produce heat for photothermal therapy, and release the PS, chlorin-6. Following release, chlorin-6 interacts with oxygen in surrounding tissues to generate reactive oxygen species for PDT.

Han *et al.* (306) engineered a chimeric peptide, PAPP-DMA, for targeted uptake by cells in the acidic TME. The peptide contains PpIX conjugated to a nuclear localization sequence (NLS) that has been modified with a negatively charged 2,3-dimethylmaleic anhydride (DMA). DMA detaches in acidic pH, increasing the charge of the peptide. This charge increase potentiates higher electrostatic interactions with the negatively charged cell membrane, facilitating internalization of the drug. Following cellular uptake, subcellular targeting of the nucleus is achieved through the NLS. This targeting strategy employs multiple layers of specificity to achieve cellular uptake in acidic conditions, as well as subcellular specificity to translocate the PS to the nucleus for light-activated DNA damage. Gao *et al.* (307) also leveraged a masked targeting peptide to target the acidic TME. They decorated the surface of a PS-loaded polymeric nanoparticle with TAT, a cell-penetrating peptide (308). To create specificity for low pH, the TAT peptide was modified with 2,3-dimethylmaleic anhydride to mask the cell-penetrating activity. Acidic pH reactivates the peptide's targeting activity, facilitating nanoparticle internalization by cells in the TME. Overall, these studies illustrate that biochemical interactions between the acidic TME and drug delivery vehicles can be leveraged to enable improved drug delivery to tumors.

## Targeted Delivery

While PSs are potent cytotoxic agents, for many formulations, clinical translation is limited by their hydrophobic nature. This causes the drugs to aggregate, thereby limiting ROS production and decreasing cytotoxicity (236). Conjugating PSs to nanoscale carriers can improve their solubility, facilitating effective delivery to, and uptake by, target cells. Nanotechnology has therefore advanced PDT by providing a mechanism to improve PS delivery. In addition to providing a vehicle for PS delivery, nanoparticle carriers can also be functionalized to specifically target cancer cells and cancer-associated stromal cells. This strategy, termed *targeted delivery*, refers to the use of antibodies as nanocarriers and targeting moieties, or the functionalization of nanocarriers and PSs with targeting moieties, to achieve specific PS delivery. This method of targeting leverages the expression of molecular biomarkers on target cells that are less expressed on other cells to selectively enhance PS accumulation and decrease systemic toxicity.

**Photoimmunotherapy.**—PIT is a form of targeted PDT that leverages the molecular targeting capabilities of antibodies and the selective phototoxicity of PSs to achieve cell-specific drug delivery (Figure 7a, 7b). This is achieved through the synthesis of photoimmunoconjugates (PICs), which are drug conjugates composed of antibodies and PSs. Cell targeting is typically dependent on the presence of membrane proteins that are differentially expressed on diseased versus normal tissue (309). Ideally, these membrane proteins should have lower expression, or none at all, on healthy cells in order to maximize specificity and minimize systemic toxicity. An antibody binding to a target can trigger receptor-mediated endocytosis, followed by proteolytic cleavage to degrade the conjugate and release the PS (310). Subsequent light irradiation leads to phototoxicity (Figure 7a) (309). Some of the cell surface receptors that serve as targets for PIT are also implicated in metastasis and proliferation. Depending on the dose, binding of the PIC can also inhibit activation of these pathways. Therefore, PICs can serve dual functions through receptor inhibition and selective delivery of the PS for PDT (311).

PIT was first described in 1983 in the lab of Julia Levy by Mew *et al.* (312). It was discovered that by conjugating the PS, hematoporphyrin, to monoclonal antibodies specific for myosarcoma, it was possible to more significantly inhibit cancer growth *in vivo* than treatment with either monotherapy alone, as well as treatment with the unconjugated antibody and PS, where all groups were light-activated. This study demonstrated for the first time that PICs can selectively enhance photodestruction of tumors. This discovery led to the development of many PICs incorporating a variety of antibody-PS combinations (84, 85, 313–315).

For example, in elegant work by Savellano and colleagues (316), the PIC conjugation and purification processes were optimized to produce highly pure PICs composed of the EGFR-specific antibody, C225, and the PS, BPD. Their optimization overcame previous issues with PIC development, including large amounts of impurities (unconjugated PSs), as well as the presence of insoluble aggregates. These issues presented a significant problem for earlier studies, because the therapeutic effects of the PICs cannot be clearly distinguished from the effects of the aggregates and impurities (316). In another study, Mitsunaga *et al.* (317)

synthesized PICs composed of EGFR-specific monoclonal antibodies (trastuzumab and panitumumab) and the PS, IRDye 700DX (IR700). It was shown that cytotoxicity was only conferred to EGFR-expressing target cells, demonstrating the selectivity of the conjugate. The authors hypothesized that fluorescence generated from light-activation of the PIC could be used for theranostic applications. Similarly, Spring and colleagues used the Cetuximab-BPD PIC developed by Savellano and colleagues to target EGFR expressing ovarian cancer micrometastases. In this PIC, the BPD molecules are self-quenched and not photoactivatable until they are internalized and proteolytically cleaved in target cells, further enhancing PIT selectivity and limiting off-target toxicity (318).

PIT has also been shown to trigger host anti-tumor immunity. A recent study by Ogawa et al. (319) explored a mechanistic understanding of cell death following PIT with mAb-IR700 PICs. The authors suggest that, unlike conventional PDT which is dependent on the generation of reactive oxygen species, cytotoxicity induced from PIT using near infrared light (NIR-PIT) is a result of membrane destabilization followed by water influx and cell bursting. This also elicits the maturation of immature dendritic cells, creating a concurrent immunological response to the tumor. A follow-up study was conducted to explore the cause of membrane destabilization (320). It was shown that upon activation with NIR light, axial ligands on IR700 dissociate, decreasing the hydrophilicity of the dye. The authors postulate a conformational change in PIC-antigen complexes following PIT that confers stress to the cell membrane, resulting in water influx and cell bursting.

While PIT has been primarily targeted to malignant cells, it can also be used to target cancer-associated stromal components in the TME. For example, work by Zhen *et al.* (321) demonstrates that CAFs can be targeted using PIT. CAFs are present in the tumor stroma and support tumor growth and metastasis by remodeling the ECM and secreting growth factors, cytokines, and chemokines (322). In this study, ferritin, which serves as a cage for the PS, ZnF16Pc, is coated with fibroblast-activation protein (FAP)-specific single chain variable fragment (scFv) to target FAP, a protein overexpressed on the surface of CAFs. One particular feature of CAFs that the authors were interested in studying was CAF-mediated T cell exclusion. By this mechanism, CAFs are able to prevent T cells from reaching the tumor through either the deposition of a dense ECM, or the production of CXCL12. It was found that CAF-targeted PIT led to a significant increase in T cell infiltration into the tumor, demonstrating that PIT can be used to modulate the tumor stroma and potentiate an immune response (Figure 7b). Importantly, the ECM deposited by CAFs is also known to provide a critical barrier to nanoparticle delivery to tumor cells (323). Therefore, Li *et al.* (324) investigated the effect of CAF-targeted PIT on nanoparticle delivery to 4T1 tumors. The authors found that by treating with CAF-targeted PIT two days prior to nanoparticle injection, intratumoral nanoparticle accumulation was improved in a particle size-dependent manner. While the effects of CAF-targeted PIT on stromal properties have been investigated, more work is required to evaluate the impact of these treatments on the mechanical properties of the TME, as well as the inverse.

While PIT is a powerful tool for targeted PS delivery, PICs have several limitations, including a relatively low PS-to-antibody ratio (typically 2 to 7 PSs per Ab), poor intracellular PIC accumulation, and limited target presentation on cells. However, PIT can be

interfaced with nanotechnology to overcome these limitations. We have previously shown that multiple PICs can be conjugated to nanoparticles (PIC-NP) for enhanced PIC uptake, as has been shown in ovarian cancer and glioblastoma cells (325). PIC-NP increases the intracellular accumulation of PIC in cancer cells by at least two-fold compared to PIC alone, which was attributed by the authors to the “carrier effect”. This phenomenon describes the indirect endocytosis of multiple PICs that are conjugated to the nanoparticle surface. Therefore, one binding event between an antibody and a target cell leads to the uptake of multiple antibodies, each with multiple PSs. This study suggests a promising direction for the future of PIT by providing a mechanism to overcome key limitations of PICs.

#### **Modified nanocarriers for cancer cell and stromal cell targeting.—**

Nanotechnology-assisted PS delivery to tumors relies on the passive accumulation of PS-nanoparticle conjugates due to the EPR effect, which is discussed in an earlier section of this review. However, upon accumulation at the tumor site, the PS can interact nonspecifically with cells in the TME. To achieve higher specificity for target cells and avoid damage to nearby healthy tissue, nanoparticle surfaces have been functionalized with various targeting moieties for molecular recognition. Similar to PIT, these functionalized nanoparticles rely on the high expression of molecular targets on the surface of target cells for specific delivery (Figure 8a). Targeting moieties used for this purpose include folic acid, peptides, antibodies, and carbohydrates (325–338) (Table 3), and can be either conjugated to a nanoparticle or directly to a PS.

Most PDT treatments that incorporate such targeting moieties are designed to directly target cancer cells. Selectively killing cancer cells can attenuate growth-induced solid stress, which is generated through interactions between structural components of the microenvironment, as discussed in previously (25).

By attenuating growth-induced solid stress, cancer cell targeting can modulate the mechanical properties of the TME. Additionally, as outlined previously, the noncancerous cellular components of the stroma can contribute to cancer progression and the mechanical stresses on the tumor. For example, CAFs and TAMs play key roles in tumor evolution through increasing malignant potential and chemoresistance (339). The noncancerous cells in the tumor stroma are therefore attractive targets for cancer therapies, and PS delivery vehicles have been designed with targeting moieties against non-cancerous stromal cells.

One method for cancer cell targeting is using carbohydrates as targeting moieties. Carbohydrates have a high binding affinity to lectins, which are endogenously overexpressed on the surface of cancer cells as well as non-cancerous stromal cells (340). A recent study in 2018 by García Calavia *et al.* (328) demonstrated that carbohydrates can serve dual functions as both targeting moieties and nanoparticle stabilizers. The investigators synthesized gold nanoparticles conjugated to zinc phthalocyanine, and the carbohydrate, lactose. Here, lactose conjugated to the surface was effective as a targeting moiety for the galectin-1 receptor on breast cancer cells, and also helped to stabilize the nanoparticle in aqueous solutions. This is an example of “direct lectin targeting”, where an exogenous carbohydrate is incorporated into the drug delivery system to target endogenously expressed carbohydrates. The binding affinity between carbohydrates and lectins can also be leveraged

by decorating the nanoparticle surface with lectins in order to target carbohydrates overexpressed on the surface of cancer cells. This strategy is termed “reverse lectin targeting” (341). The latter strategy was investigated in a study by Obaid *et al.* (331) that compared using lectin for carbohydrate-targeted nanoparticles with using antibodies for protein receptor-targeted nanoparticles. To study this, gold nanoparticles were functionalized with either the lectin, jacalin, or a monoclonal antibody. Both constructs used zinc phthalocyanine (C11Pc) as the PS, and efficacy of the constructs was evaluated in multiple cancer cell lines: HT-29 colon cancer cells and SK-BR-3 breast cancer cells. Here, the jacalin was used to target the cell surface molecule Thomsen–Friedenreich carbohydrate antigen (T antigen), and the monoclonal antibody was specific to HER-2. Results from this study demonstrated that PDT toxicity *in vitro* was comparable between both conjugates in both cancer cell lines, illustrating that targeting carbohydrates with lectins and targeting transmembrane proteins with antibodies can elicit similar toxicities when combined with PDT. The authors suggest that this outcome may be explained by the different binding affinities and cell surface receptor densities. While the dissociation constant of jacalin binding to HT-29 cells is higher than that of anti-HER-2 antibodies binding to SK-BR-3 cells, the HT-29 expression of T-antigen is higher than the SK-BR-3 expression of HER-2 receptors. Thus, both binding affinity and target expression are critical parameters for the design of targeted nanotherapeutics.

Another common targeting moiety that is used to decorate the surface of nanoparticles is folate, which specifically targets folate receptors (332–334). The folate receptor is a GPI-anchored cell surface receptor that is overexpressed in many cancers, making it an attractive receptor for targeted therapies (342). The receptor is responsible for mediating the intracellular transport of folate via receptor-mediated endocytosis. In a study by Kato *et al.* (332), folate receptor-targeted porphyrins were synthesized and studied as a lung cancer treatment *in vitro* and *in vivo*. In an orthotopic lung tumor model, both the non-targeted porphyrins and folate-targeted porphyrins (FPs) had higher accumulation in the tumor compared to the healthy lung tissue, but FP administration led to higher intracellular PS accumulation. This study illustrates that nanoparticles with and without targeting moieties are able to accumulate preferentially at the tumor, but the targeting moieties are key for improving uptake by target cells.

Similarly, peptides can also be conjugated to the nanoparticle surface to achieve tumor-specific drug delivery. The use of peptides for targeting has several potential benefits over antibodies, including lower risk of immune reactivity, smaller size, high stability, and simple synthesis (343, 344). In a study by Sebak *et al.* (335), the peptide, cyclic (Arginine-Glycine-Aspartic acid-D-Tyrosine-Lysine) (cRGDyk), was conjugated to poly(lactic-co-glycolic acid) (PLGA) nanoparticles. The cRGDyk peptide served dual functions in this construct as both a targeting moiety and a quenching agent. Quenching agents like this are attractive features for PDT because they attenuate singlet oxygen generation outside of the tumor site, thereby improving specificity and limiting off-target cytotoxicity (345). In another study, Gao *et al.* (346) investigated the effects of  $\alpha\beta_6$  integrin-targeted PDT on host immune response. The authors demonstrated that integrin-targeted PDT using IRDye700-streptavidin-biotin-HK peptide (DSAB-HK) could both inhibit tumor growth and stimulate the host anti-tumor response by promoting dendrite maturation and T lymphocyte

recruitment. While PDT can be used to target integrins for cancer cell destruction, PDT has also been shown to modulate integrin expression in cancer cells. One study showed a significant reduction in the protein and mRNA expression of FAK and  $\beta 1$ -integrin 12 hours after PDT (347). Similarly, Runnels and colleagues have shown that BPD-mediated PDT at a mild dose ( $0.5 \text{ J cm}^{-2}$ ) induces the loss of  $\beta 1$  integrin-containing focal adhesion plaques (162). Because BPD was shown to localize in the mitochondria with no marked fluorescence at the membrane, and  $\beta 1$ -containing integrins seemed to be structurally intact after photosensitization, the authors suggest that the PDT-mediated loss of integrin function occurred through intracellular damage rather than direct photodamage.

While the vast majority of targeted PDT strategies have focused on targeting cancer cells, there are a variety of stromal cells that contribute to cancer progression, as discussed in a previous section. TAMs are known to promote cancer proliferation and metastasis through a variety of mechanisms including inflammatory cytokine release, increased angiogenesis, suppression of T cell response, and ECM remodeling (348, 349). Due to the role of TAMs in ECM remodeling, strategies that target these tumor-promoting immune cells could potentially impact the stiffness of the TME.

Previous work by Hayashi *et al.* (329) has demonstrated that PDT can be used to target TAMs. The authors synthesized mannose-conjugated chlorin (M-chlorin) to target the overexpressed mannose receptors on TAMs (Figure 8b). While these constructs were initially designed for specific toxicity in TAMs and not cancer cells, it was found that M-chlorin-PDT conferred cytotoxicity to tumor cells to a similar degree *in vitro* as the cancer cell-targeted control, glucose-conjugated chlorin (G-chlorin). This was attributed to the expression of mannose receptors on cancer cells. However, *in vivo* studies showed that M-chlorin PDT led to significantly more tumor suppression than G-chlorin PDT, which was attributed to the affinity of M-chlorin for CD-206 expressing TAMs in addition to cancer cells. These results suggest exciting opportunities for future studies that target multiple cell types with a single targeting moiety to achieve enhanced anti-tumor effect. Such constructs could potentially achieve synergistic cytotoxicity by killing cancer cells as well as the non-malignant cells that contribute to tumor maintenance, thereby providing an inherent mechanism for managing the cancer cells that survive initial treatment. Similarly, Wen and colleagues used a natural noninfectious nanocarrier, cowpea mosaic virus (CPMV), to target TAMs (74). CPMV has been shown to have a preference for M2-polarized macrophages. However, they also have affinity for vimentin, which is overexpressed in certain epithelial cancers, including prostate cancer, gastrointestinal tumors, breast cancer, and lung cancer (350). According to the results of the study, the PS-CPMV nanoconstruct (zinc ethynylphenyl porphyrin conjugated CPMV/ dendron hybrid) was effective on both cancer cells and macrophages but did not favor the M2 subpopulation, despite previous work suggesting that CPMV has a preference for M2-polarized macrophages (74).

## CONCLUSION

PDT- and PIT-based treatments and combination regimens provide several advantages over conventional agents. These advantages include distinct cytotoxic mechanisms and dual selectivity achieved via both spatiotemporal control of light and PS targeting. An area that

remains understudied in the design of targeted PDT and multi-agent combinations is the role of mechanical stress and the stromal components in the TME. This can include the destruction of cellular components such as CAFs and TAMs or degradation of noncellular components to modulate mechanical stresses and alter the TME. Controlled alterations in the tumor architecture and stiffness could enhance cytotoxic effects due to the role of the TME in promoting a variety of survival pathways in tumors (351).

Previous studies exploring targeting strategies against CAFs and TAMs, including by PDT, (321–324), (336), (348, 349) have demonstrated the potential to regulate the TME and modulate stiffness. These findings have implications for enhanced immune response (e.g. T cell infiltration) and drug delivery (321–324). Further work could explore how PDT-mediated targeting of CAFs and TAMs impacts metastatic potential and cell motility by remodeling the TME. This review also addresses the potential of PDT to modulate noncellular components of tumor ECM, such as collagen and hyaluronic acid. Although remodeling of the ECM seems promising for decreasing mechanical stress in the TME, the degradation of such components may also have unwanted outcomes, such as promoting invasiveness and migration of cancer cells, emphasizing the need for improved understanding and careful design of targeted regimens.

This review divides targeted PDT into three main categories: *targeting through by cellular and tissue modulation*, *functional targeting*, and *targeted delivery*. However, many of the categories can be combined to cooperatively achieve improved treatment outcomes depending on the target site. For example, many nanoparticle treatments that require intravenous injection will likely accumulate at the tumor site passively due to the EPR effect, underscoring the critical role that *functional targeting* can have for a variety of cancer treatments. Additionally, *cellular and tissue modulation* strategies can be utilized to prime a tumor for another targeted treatment strategy to enhance PDT efficacy. Therefore, the future of targeted PDT is not necessarily in one singular strategy, but rather the development of highly targeted treatment plans that leverage multiple routes to achieve specific and potent drug delivery.

Figure 9 summarizes the complexity of the relationships between mechanical stress and the TME components that have been reviewed here. Many components of the TME and mechanical stress are inter-related, highlighting the importance of rationally-designed targeted PDT combination that exploit and modulate the TME with the goal of enhanced tumor destruction and inhibition of metastases. Future work could also focus on using PDT to target other cell types that are present in the stroma and implicated in promoting tumor growth and metastasis. Strategies that simultaneously target cancer cells and the tumor-promoting noncancerous cells have been explored as well (329), and there is immense potential for further studies in this area.

## ACKNOWLEDGEMENTS

In memory of our colleague, Dr. Jarod Finlay. He was a valued member of our community who made important contributions to PDT and photobiology. His work advanced our understanding of tissue optical properties, light propagation and dosimetry, photosensitizer photobleaching, and tumor hemodynamics. He will be missed.

This work is supported by the following funding sources:

Dr. William Polacheck - NC Translational and Clinical Sciences Institute (NCTraCS), supported by the National Center for Advancing Translational Sciences (NCATS), National Institutes of Health (NIH), through Grant Award Number UL1TR002489, and UNC-NCSU Joint BME Department Start-up Fund.

Dr. Jonathan Celli – NIH U54CA156734 UMass Boston-Dana Farber/Harvard Cancer Center Partnership

Dr. Huang-Chiao Huang - NIH R00CA194269, UMD Start-up Fund, UMD-UMB 2018 Research and Innovation Seed Grant, the Caring Together, NY, Ovarian Cancer Research grant, and the UMD-NCI Partnership for Integrative Cancer Research Grant.

Dr. Imran Rizvi - NIH R00CA175292, NC TraCS, NIH UL1TR002489, and UNC-NCSU Joint BME Department Start-up Fund.

## ABBREVIATIONS

<b>5-ALA</b>	5-aminolevulinic acid
<b>AMD</b>	age-related macular degeneration
<b>BPD</b>	benzoporphyrin derivative
<b>CAF</b>	cancer-associated fibroblast
<b>CNV</b>	choroidal neovascularization
<b>CPMV</b>	cowpea mosaic virus
<b>CPO</b>	coproporphyrinogen
<b>DMA</b>	2,3-dimethylmaleic anhydride
<b>ECM</b>	extracellular matrix
<b>EGFR</b>	epidermal growth factor receptor
<b>EMT</b>	epithelia-mesenchymal transition
<b>EPR</b>	enhanced permeability and retention
<b>FAP</b>	fibroblast-activation protein
<b>FDA</b>	U. S. Food and Drug Administration
<b>FECH</b>	ferrochelatase
<b>HIF</b>	hypoxia-inducible factor
<b>IFP</b>	interstitial fluid pressure
<b>L-PDT</b>	low-dose photodynamic therapy
<b>MMP</b>	matrix metalloproteinase
<b>NLS</b>	nuclear localization sequence
<b>NMAPS</b>	nonmembrane anchoring photosensitizer
<b>OVV</b>	oncolytic vaccinia virus

<b>PDT</b>	photodynamic therapy
<b>pHLIP</b>	pH low insertion peptide
<b>pHMAPS</b>	pH-driven membrane anchoring photosensitizer
<b>PIC</b>	photoimmunoconjugate
<b>PIT</b>	photoimmunotherapy
<b>PpIX</b>	protoporphyrin IX
<b>PS</b>	photosensitizer
<b>PTT</b>	photothermal therapy
<b>TAM</b>	tumor-associated macrophage
<b>TGF-<math>\beta</math></b>	transforming growth factor- $\beta$
<b>TME</b>	tumor microenvironment
<b>TPZ</b>	tirapazamine
<b>VEGF</b>	vascular endothelial growth factor
<b>ZnPc</b>	Zinc phthalocyanine

## REFERENCES

1. Zhu TC and Finlay JC (2008) The role of photodynamic therapy (PDT) physics. *Med. Phys* 35, 3127–3136. [PubMed: 18697538]
2. Celli JP, Spring BQ, Rizvi I, Evans CL, Samkoe KS, Verma S, Pogue BW and Hasan T (2010) Imaging and Photodynamic Therapy: Mechanisms, Monitoring and Optimization. *Chem. Rev* 110, 2795–2838. [PubMed: 20353192]
3. Agostinis P, Berg K, Cengel KA, Foster TH, Girotti AW, Gollnick SO, Hahn SM, Hamblin MR, Juzeniene A, Kessel D, Korbelik M, Moan J, Mroz P, Nowis D, Piette J, Wilson B and Golab J (2011) Photodynamic Therapy of Cancer: An Update. *CA. Cancer J. Clin* 61, 250–281. [PubMed: 21617154]
4. Kessel D and Oleinick NL (2018) Cell Death Pathways Associated with Photodynamic Therapy: An Update. *Photochem. Photobiol* 94, 213–218. [PubMed: 29143339]
5. Oleinick NL, Morris RL and Belichenko I (2002) The role of apoptosis in response to photodynamic therapy: What, where, why, and how. *Photochem. Photobiol. Sci* 1, 1–21. [PubMed: 12659143]
6. Goler-Baron V and Assaraf YG (2012) Overcoming multidrug resistance via photodestruction of ABCG2-rich extracellular vesicles sequestering photosensitive chemotherapeutics. *PLoS One* 7, e35487–e35487. [PubMed: 22530032]
7. Brown SB, Brown EA and Walker I (2004) The present and future role of photodynamic therapy in cancer treatment. *Lancet Oncol.* 5, 497–508. [PubMed: 15288239]
8. Spring BQ, Rizvi I, Xu N and Hasan T (2016) The role of photodynamic therapy in overcoming cancer drug resistance. *Photochem. Photobiol. Sci* 14, 1476–1491.
9. Dougherty TJ, Gomer CJ, Henderson BW, Jori G, Kessel D, Korbelik M, Moan J and Peng Q (1998) Photodynamic therapy. *J. Natl. Cancer Inst* 90, 889–905. [PubMed: 9637138]
10. Castano AP, Mroz P and Hamblin MR (2006) Photodynamic therapy and anti-tumour immunity. *Nat. Rev. Cancer* 6, 535–545. [PubMed: 16794636]

11. Nath S, Obaid G and Hasan T (2019) The Course of Immune Stimulation by Photodynamic Therapy: Bridging fundamentals of photochemically-induced Immunogenic Cell Death to the Enrichment of T Cell Repertoire. *Photochem. Photobiol* doi: 10.1111/php.13173.
12. Anand S, Ortel BJ, Pereira SP, Hasan T and Maytin EV (2012) Biomodulatory approaches to photodynamic therapy for solid tumors. *Cancer Lett.* 326, 8–16. [PubMed: 22842096]
13. Niu CJ, Fisher C, Scheffler K, Wan R, Maleki H, Liu H, Sun Y, A. Simmons C, Birngruber R and Lilge L (2015) Polyacrylamide gel substrates that simulate the mechanical stiffness of normal and malignant neuronal tissues increase protoporphyrin IX synthesis in glioma cells. *J. Biomed. Opt* 20, 1–7.
14. Naves LB, Ramakrishna S, Venugopal JR, Rajamani L, Almeida L and Dhand C (2017) Nanotechnology for the treatment of melanoma skin cancer. *Prog. Biomater* 6, 13–26. [PubMed: 28303522]
15. Ingber DE (1997) Tensegrity: The Architectural Basis of Cellular Mechanotransduction. *Annu. Rev. Physiol* 59, 575–599. [PubMed: 9074778]
16. Ingber DE (2003) Tensegrity II. How structural networks influence cellular information processing networks. *J. Cell Sci* 116, 1397 LP–1408. [PubMed: 12640025]
17. Polacheck WJ, German AE, Mammoto A, Ingber DE and Kamm RD (2014) Mechanotransduction of fluid stresses governs 3D cell migration. *Proc. Natl. Acad. Sci* 111, 2447–2452. [PubMed: 24550267]
18. Galbraith CG, Yamada KM and Sheetz MP (2002) The relationship between force and focal complex development. *J. Cell Biol* 159, 695–705. [PubMed: 12446745]
19. Northcott JM, Dean IS, Mouw JK and Weaver VM (2018) Feeling Stress: The Mechanics of Cancer Progression and Aggression. *Front. Cell Dev. Biol* 6, 1–12. [PubMed: 29417046]
20. Nia HT, Liu H, Seano G, Datta M, Jones D, Rahbari N, Incio J, Chauhan VP, Jung K, Martin JD, Askoxylakis V, Padera TP, Fukumura D, Boucher Y, Hornicek FJ, Grodzinsky AJ, Baish JW, Munn LL and Jain RK (2017) Solid stress and elastic energy as measures of tumour mechanopathology. *Nat. Biomed. Eng* 1, 1–25.
21. Stylianopoulos T, Martin JD, Chauhan VP, Jain SR, Diop-Frimpong B, Bardeesy N, Smith BL, Ferrone CR, Hornicek FJ, Boucher Y, Munn LL and Jain RK (2012) Causes, consequences, and remedies for growth-induced solid stress in murine and human tumors. *Proc. Natl. Acad. Sci* 109, 15101–15108. [PubMed: 22932871]
22. Cheng G, Tse J, Jain RK and Munn LL (2009) Micro-environmental mechanical stress controls tumor spheroid size and morphology by suppressing proliferation and inducing apoptosis in cancer cells. *PLoS One* 4, 1–11.
23. Helmlinger G, Netti PA, Lichtenbeld HC, Melder RJ and Jain RK (1997) Solid stress inhibits the growth of multicellular tumor spheroids. *Nat. Biotechnol* 15, 778–783. [PubMed: 9255794]
24. Jain RK, Martin JD and Stylianopoulos T (2014) The role of mechanical forces in tumor growth and therapy. *Annu. Rev. Biomed. Eng* 16, 321–346. [PubMed: 25014786]
25. Kalli M and Stylianopoulos T (2018) Defining the Role of Solid Stress and Matrix Stiffness in Cancer Cell Proliferation and Metastasis. *Front. Oncol* 8, 1–7. [PubMed: 29404275]
26. Demou ZN (2010) Gene expression profiles in 3D tumor analogs indicate compressive strain differentially enhances metastatic potential. *Ann. Biomed. Eng* 38, 3509–3520. [PubMed: 20559731]
27. Tse JM, Cheng G, Tyrrell JA, Wilcox-Adelman SA, Boucher Y, Jain RK and Munn LL (2012) Mechanical compression drives cancer cells toward invasive phenotype. *Proc. Natl. Acad. Sci* 109, 911–916. [PubMed: 22203958]
28. Mak M, Reinhart-King CA and Erickson D (2013) Elucidating mechanical transition effects of invading cancer cells with a subnucleus-scaled microfluidic serial dimensional modulation device. *Lab Chip* 13, 340–348. [PubMed: 23212313]
29. Butcher DT, Alliston T and Weaver VM (2009) A tense situation: forcing tumour progression. *Nat. Rev. Cancer* 9, 108–122. [PubMed: 19165226]
30. Alessandri K, Sarangi BR, Gurchenkov VV, Sinha B, Kiessling TR, Fetler L, Rico F, Scheuring S, Lamaze C, Simon A, Geraldo S, Vignjevic D, Domejean H, Rolland L, Funfak A, Bibette J, Bremond N and Nassoy P (2013) Cellular capsules as a tool for multicellular spheroid production

- and for investigating the mechanics of tumor progression in vitro. *Proc. Natl. Acad. Sci* 110, 14843–14848. [PubMed: 23980147]
31. Nia HT, Datta M, Seano G, Huang P, Munn LL and Jain RK (2018) Quantifying solid stress and elastic energy from excised or in situ tumors. *Nat. Protoc* 13, 1091–1105. [PubMed: 29674756]
  32. Nieskoski MD, Marra K, Gunn JR, Kanick SC, Doyley MM, Hasan T, Pereira SP, Stuart Tremblay B and Pogue BW (2017) Separation of Solid Stress From Interstitial Fluid Pressure in Pancreas Cancer Correlates With Collagen Area Fraction. *J. Biomech. Eng* 139.
  33. Roose T, Netti PA, Munn LL, Boucher Y and Jain RK (2003) Solid stress generated by spheroid growth estimated using a linear poroelasticity model. *Microvasc. Res* 66, 204–212. [PubMed: 14609526]
  34. Santinoranont M, Rooney F and Ferrari M (2003) Interstitial stress and fluid pressure within a growing tumor. *Ann. Biomed. Eng* 31, 327–335. [PubMed: 12680730]
  35. Stylianopoulos T, Martin JD, Snuderl M, Mpekris F, Jain SR and Jain RK (2013) Coevolution of solid stress and interstitial fluid pressure in tumors during progression: implications for vascular collapse. *Cancer Res* 73, 3833–3841. [PubMed: 23633490]
  36. Cramer GM, Jones DP, El-Hamidi H and Celli JP (2017) ECM Composition and Rheology Regulate Growth, Motility, and Response to Photodynamic Therapy in 3D Models of Pancreatic Ductal Adenocarcinoma. *Mol. Cancer Res* 15, 15–25. [PubMed: 27671335]
  37. Pathak A and Kumar S (2012) Independent regulation of tumor cell migration by matrix stiffness and confinement. *Proc. Natl. Acad. Sci* 109, 10334–10339. [PubMed: 22689955]
  38. Celli JP (2012) Stromal interactions as regulators of tumor growth and therapeutic response: A potential target for photodynamic therapy? *Isr. J. Chem* 52, 757–766. [PubMed: 23457416]
  39. Paszek MJ, Zahir N, Johnson KR, Lakins JN, Rozenberg GI, Gefen A, Reinhart-King CA, Margulies SS, Dembo M, Boettiger D, Hammer DA and Weaver VM (2005) Tensional homeostasis and the malignant phenotype. *Cancer Cell* 8, 241–254. [PubMed: 16169468]
  40. Barcus CE, Keely PJ, Eliceiri KW and Schuler LA (2013) Stiff collagen matrices increase tumorigenic prolactin signaling in breast cancer cells. *J. Biol. Chem* 288, 12722–12732. [PubMed: 23530035]
  41. Calvo F, Ege N, Grande-Garcia A, Hooper S, Jenkins RP, Chaudhry SI, Harrington K, Williamson P, Moeendarbary E, Charras G and Sahai E (2013) Mechanotransduction and YAP-dependent matrix remodelling is required for the generation and maintenance of cancer-associated fibroblasts. *Nat. Cell Biol* 15, 637–646. [PubMed: 23708000]
  42. Levental KR, Yu H, Kass L, Lakins JN, Egeblad M, Erler JT, Fong SFT, Csiszar K, Giaccia A, Weninger W, Yamauchi M, Gasser DL and Weaver VM (2009) Matrix Crosslinking Forces Tumor Progression by Enhancing Integrin Signaling. *Cell* 139, 891–906. [PubMed: 19931152]
  43. Lam WA, Cao L, Umesh V, Keung AJ, Sen S and Kumar S (2010) Extracellular matrix rigidity modulates neuroblastoma cell differentiation and N-myc expression. *Mol. Cancer* 9, 35. [PubMed: 20144241]
  44. Oudin MJ and Weaver VM (2016) Physical and chemical gradients in the tumor microenvironment regulate tumor cell invasion, migration, and metastasis. *Cold Spring Harb. Symp. Quant. Biol* 81, 189–205. [PubMed: 28424337]
  45. Nguyen-Ngoc K-V, Cheung KJ, Brenot A, Shamir ER, Gray RS, Hines WC, Yaswen P, Werb Z and Ewald AJ (2012) ECM microenvironment regulates collective migration and local dissemination in normal and malignant mammary epithelium. *Proc. Natl. Acad. Sci. U. S. A* 109, E2595–E2604. [PubMed: 22923691]
  46. Ulrich TA, Jain A, Tanner K, MacKay JL and Kumar S (2010) Probing cellular mechanobiology in three-dimensional culture with collagen–agarose matrices. *Biomaterials* 31, 1875–1884. [PubMed: 19926126]
  47. Ananthanarayanan B, Kim Y and Kumar S (2011) Elucidating the mechanobiology of malignant brain tumors using a brain matrix-mimetic hyaluronic acid hydrogel platform. *Biomaterials* 32, 7913–7923. [PubMed: 21820737]
  48. Gill BJ, Gibbons DL, Roudsari LC, Saik JE, Rizvi ZH, Roybal JD, Kurie JM and West JL (2012) A synthetic matrix with independently tunable biochemistry and mechanical properties to study

- epithelial morphogenesis and EMT in a lung adenocarcinoma model. *Cancer Res.* 72, 6013–6023. [PubMed: 22952217]
49. Soman P, Kelber JA, Lee JW, Wright TN, Vecchio KS, Klemke RL and Chen S (2012) Cancer cell migration within 3D layer-by-layer microfabricated photocrosslinked PEG scaffolds with tunable stiffness. *Biomaterials* 33, 7064–7070. [PubMed: 22809641]
  50. Celli JP and Anderson MDBT-RM in L. S (2017) *Cancer Biophysics In Reference Module in Life Sciences*, pp. 1–8. Elsevier.
  51. Swartz MA and Fleury ME (2007) Interstitial Flow and Its Effects in Soft Tissues. *Annu. Rev. Biomed. Eng* 9, 229–256. [PubMed: 17459001]
  52. Heldin C-H, Rubin K, Pietras K and Östman A (2004) High interstitial fluid pressure — an obstacle in cancer therapy. *Nat. Rev. Cancer* 4, 806–813. [PubMed: 15510161]
  53. Kobayashi H, Watanabe R and Choyke PL (2014) Improving conventional enhanced permeability and retention (EPR) effects; What is the appropriate target? *Theranostics* 4, 81–89.
  54. Rutkowski JM and Swartz MA (2007) A driving force for change: interstitial flow as a morphoregulator. *Trends Cell Biol.* 17, 44–50. [PubMed: 17141502]
  55. Curti BD, Urba WJ, Gregory Alvord W, Janik JE, Smith JW, Madara K and Longo DL (1993) Interstitial Pressure of Subcutaneous Nodules in Melanoma and Lymphoma Patients: Changes during Treatment. *Cancer Res.* 53, 2204 LP–2207. [PubMed: 8485703]
  56. Nathanson SD and Nelson L (1994) Interstitial fluid pressure in breast cancer, benign breast conditions, and breast parenchyma. *Ann. Surg. Oncol* 1, 333–338. [PubMed: 7850532]
  57. Provenzano PP and Hingorani SR (2013) Hyaluronan, fluid pressure, and stromal resistance in pancreas cancer. *Br. J. Cancer* 108, 1–8. [PubMed: 23299539]
  58. Hofmann M, Guschel M, Bernd A, Bereiter-Hahn J, Kaufmann R, Tandl C, Wiig H and Kippenberger S (2006) Lowering of tumor interstitial fluid pressure reduces tumor cell proliferation in a xenograft tumor model. *Neoplasia* 8, 89–95. [PubMed: 16611401]
  59. Swartz MA and Lund AW (2012) Lymphatic and interstitial flow in the tumour microenvironment: linking mechanobiology with immunity. *Nat. Rev. Cancer* 12, 210–219. [PubMed: 22362216]
  60. Yu H, Mouw JK and Weaver VM (2011) Forcing Form and Function: Biomechanical Regulation of Tumor Evolution. *Trends Cell Biol.* 21, 47–56. [PubMed: 20870407]
  61. Shields JD, Fleury ME, Yong C, Tomei AA, Randolph GJ and Swartz MA (2007) Autologous Chemotaxis as a Mechanism of Tumor Cell Homing to Lymphatics via Interstitial Flow and Autocrine CCR7 Signaling. *Cancer Cell* 11, 526–538. [PubMed: 17560334]
  62. Polacheck WJ, Charest JL and Kamm RD (2011) Interstitial flow influences direction of tumor cell migration through competing mechanisms. *Proc. Natl. Acad. Sci* 108, 11115–11120. [PubMed: 21690404]
  63. Li R, Xing H, Lee TA, Kamm RD, Serrano JC, Azizgolshani H and Zaman M (2018) Interstitial flow promotes macrophage polarization toward an M2 phenotype. *Mol. Biol. Cell* 29, 1927–1940. [PubMed: 29995595]
  64. Avvisato CL, Yang X, Shah S, Hoxter B, Li W, Gaynor R, Pestell R, Tozeren A and Byers SW (2007) Mechanical force modulates global gene expression and beta-catenin signaling in colon cancer cells. *J. Cell Sci* 120, 2672–2682. [PubMed: 17635998]
  65. Adam RA and Adam YG (2004) Malignant ascites: Past, present, and future. *J. Am. Coll. Surg* 198, 999–1011. [PubMed: 15194082]
  66. Rizvi I, Gurkan UA, Tasoglu S, Alagic N, Celli JP, Mensah LB, Mai Z, Demirci U and Hasan T (2013) Flow induces epithelial-mesenchymal transition, cellular heterogeneity and biomarker modulation in 3D ovarian cancer nodules. *PNAS* E1974–E1983.
  67. Kalluri R (2016) The biology and function of fibroblasts in cancer. *Nat. Rev. Cancer* 16, 582–598. [PubMed: 27550820]
  68. Joyce J and Quail D (2013) Microenvironmental regulation of tumor progression and metastasis. *Nat. Med* 19, 1423–1437. [PubMed: 24202395]
  69. Shao ZM, Nguyen M and Barsky SH (2000) Human breast carcinoma desmoplasia is PDGF initiated. *Oncogene* 19, 4337–4345. [PubMed: 10980609]

70. Bremnes RM, Dønnem T, Al-Saad S, Al-Shibli K, Andersen S, Sirera R, Camps C, Marinez I and Busund LT (2011) The role of tumor stroma in cancer progression and prognosis: Emphasis on carcinoma-associated fibroblasts and non-small cell lung cancer. *J. Thorac. Oncol* 6, 209–217. [PubMed: 21107292]
71. Kalluri R and Zeisberg M (2006) Fibroblasts in cancer. *Nat. Rev. Cancer* 6, 392–401. [PubMed: 16572188]
72. Choi H and Moon A (2018) Crosstalk between cancer cells and endothelial cells: implications for tumor progression and intervention. *Arch. Pharm. Res* 41, 711–724. [PubMed: 29961196]
73. Koukourakis MI, Giatromanolaki A, Harris AL and Sivridis E (2006) Comparison of Metabolic Pathways between Cancer Cells and Stromal Cells in Colorectal Carcinomas: a Metabolic Survival Role for Tumor-Associated Stroma. *Cancer Res.* 66, 632 LP–637. [PubMed: 16423989]
74. Wen AM, Lee KL, Cao P, Pangilinan K, Carpenter BL, Lam P, Veliz FA, Ghiladi RA, Advincula RC and Steinmetz NF (2016) Utilizing Viral Nanoparticle/Dendron Hybrid Conjugates in Photodynamic Therapy for Dual Delivery to Macrophages and Cancer Cells. *Bioconjug. Chem* 27, 1227–1235. [PubMed: 27077475]
75. Pathria P, Louis TL and Varner JA (2019) Targeting Tumor-Associated Macrophages in Cancer. *Trends Immunol.* 40, 310–327. [PubMed: 30890304]
76. Zeisberg EM, Potenta S, Xie L, Zeisberg M and Kalluri R (2007) Discovery of Endothelial to Mesenchymal Transition as a Source for Carcinoma-Associated Fibroblasts. *Cancer Res.* 67, 10123 LP–10128. [PubMed: 17974953]
77. David CJ and Massagué J (2018) Contextual determinants of TGF $\beta$  action in development, immunity and cancer. *Nat. Rev. Mol. Cell Biol* 19, 419–435. [PubMed: 29643418]
78. Xu J, Lamouille S and Derynck R (2009) TGF-beta-induced epithelial to mesenchymal transition. *Cell Res.* 19, 156–172. [PubMed: 19153598]
79. Yoshida GJ, Azuma A and Miura Y (2019) Activated Fibroblast Program Orchestrates Tumor Initiation and Progression ; Molecular Mechanisms and the Associated Therapeutic Strategies. *Int. J. Mol. Sci* 20, 1–30.
80. Bhowmick NA, Neilson EG and Moses HL (2004) Stromal fibroblasts in cancer initiation and progression. *Nature* 432, 332–337. [PubMed: 15549095]
81. Biernacka A, Dobaczewski M and Frangogiannis NG (2011) TGF- $\beta$  signaling in fibrosis. *Growth Factors* 29, 196–202. [PubMed: 21740331]
82. Mantovani A, Marchesi F, Malesci A, Laghi L and Allavena P (2017) Tumour-associated macrophages as treatment targets in oncology. *Nat. Rev. Clin. Oncol* 14, 399–416. [PubMed: 28117416]
83. Gabrilovich D, Ishida T, Oyama T, Ran S, Kravtsov V, Nadaf S and Carbone DP (1998) Vascular endothelial growth factor inhibits the development of dendritic cells and dramatically affects the differentiation of multiple hematopoietic lineages in vivo. *Blood* 92, 4150–66. [PubMed: 9834220]
84. Dikov MM, Ohm JE, Ray N, Tchekneva EE, Burlison J, Moghanaki D, Nadaf S and Carbone DP (2014) Differential Roles of Vascular Endothelial Growth Factor Receptors 1 and 2 in Dendritic Cell Differentiation. *J. Immunol* 174, 215–222.
85. Walker C, Mojares E and del Río Hernández A (2018) Role of Extracellular Matrix in Development and Cancer Progression. *Int. J. Mol. Sci* 19, 1–31.
86. Lu P, Weaver VM and Werb Z (2012) The extracellular matrix: A dynamic niche in cancer progression. *J. Cell Biol* 196, 395–406. [PubMed: 22351925]
87. Haddow A (1973) Molecular Repair, Wound Healing, And Carcinogenesis: Tumor Production A Possible Overhealing? *Adv Cancer Res.* 16, 181–234.
88. Dvorak HF (1986) Tumors: Wounds That Do Not Heal. *N. Engl. J. Med* 315, 1650–1659. [PubMed: 3537791]
89. Ziani L, Chouaib S and Thiery J (2018) Alteration of the antitumor immune response by cancer-associated fibroblasts. *Front. Immunol* 9, 1–14. [PubMed: 29403488]
90. Michael W.P, Mouw JK and Weaver VM (2014) The extracellular matrix modulates the hallmarks of cancer Michael. *EMBO Rep.* 15, 1243–1253. [PubMed: 25381661]
91. Pazos MDC and Nader HB (2007) Effect of photodynamic therapy on the extracellular matrix and associated components. *Brazilian J. Med. Biol. Res* 40, 1025–1035.

92. Giancotti FG and Ruoslahti E (1999) Integrin Signaling. *Science* (80-. ). 285, 1028 LP–1033.
93. Desgrosellier JS and Cheresch DA (2010) Integrins in cancer: biological implications and therapeutic opportunities. *Nat. Rev. Cancer* 10, 9–22. [PubMed: 20029421]
94. Guo W and Giancotti FG (2004) Integrin signalling during tumour progression. *Nat. Rev. Mol. Cell Biol* 5, 816–826. [PubMed: 15459662]
95. Attieh Y, Clark AG, Grass C, Richon S, Pocard M, Mariani P, Elkhatib N, Betz T, Gurchenkov B and Vignjevic DM (2017) Cancer-associated fibroblasts lead tumor invasion through integrin- $\beta$ 3-dependent fibronectin assembly. *J. Cell Biol* 216, 3509–3520. [PubMed: 28931556]
96. Seguin L, Kato S, Franovic A, Camargo MF, Lesperance J, Elliott KC, Yebra M, Mielgo A, Lowy AM, Husain H, Cascone T, Diao L, Wang J, Wistuba II, Heymach JV, Lippman SM, Desgrosellier JS, Anand S, Weis SM and Cheresch DA (2014) An integrin  $\beta$ <sub>3</sub>-KRAS-RalB complex drives tumour stemness and resistance to EGFR inhibition. *Nat. Cell Biol* 16, 457–468. [PubMed: 24747441]
97. Hamidi H and Ivaska J (2018) Every step of the way: integrins in cancer progression and metastasis. *Nat. Rev. Cancer* 18, 533–548. [PubMed: 30002479]
98. Wilson WR and Hay MP (2011) Targeting hypoxia in cancer therapy. *Nat. Rev. Cancer* 11, 393–410. [PubMed: 21606941]
99. Muz B, de la Puente P, Azab F and Azab AK (2015) The role of hypoxia in cancer progression, angiogenesis, metastasis, and resistance to therapy. *Hypoxia* 3, 83–92. [PubMed: 27774485]
100. Vaupel P and Harrison L (2004) Tumor Hypoxia: Causative Factors, Compensatory Mechanisms, and Cellular Response. *Oncologist* 9, 4–9.
101. Roma-Rodrigues Catarina, Mendes Rita, Baptista Pedro V., F. AR (2019) Targeting the tumor microenvironment for cancer therapy. *Int. J. Mol. Sci* 20, 1–31.
102. Semenza GL (2003) Targeting HIF-1 for cancer therapy. *Nat. Rev. Cancer* 3, 721–732. [PubMed: 13130303]
103. Azab AK, Hu J, Quang P, Azab F, Pitsillides C, Awwad R, Thompson B, Maiso P, Sun JD, Hart CP, Roccaro AM, Sacco A, Ngo HT, Lin CP, Kung AL, Carrasco RD, Vanderkerken K and Ghobrial IM (2012) Hypoxia promotes dissemination of multiple myeloma through acquisition of epithelial to mesenchymal transition-like features. *Blood* 119, 5782–5794. [PubMed: 22394600]
104. Iyer AK, Khaled G, Fang J and Maeda H (2006) Exploiting the enhanced permeability and retention effect for tumor targeting. *Drug Discov. Today* 11, 812–818. [PubMed: 16935749]
105. Siemann DW (2011) The unique characteristics of tumor vasculature and preclinical evidence for its selective disruption by Tumor-Vascular Disrupting Agents. *Cancer Treat. Rev* 37, 63–74. [PubMed: 20570444]
106. Maeda H (2001) The enhanced permeability and retention (EPR) effect in tumor vasculature: The key role of tumor-selective macromolecular drug targeting. *Adv. Enzyme Regul* 41, 189–207. [PubMed: 11384745]
107. Ngoune R, Peters A, von Elverfeldt D, Winkler K and Pütz G (2016) Accumulating nanoparticles by EPR: A route of no return. *J. Control. Release* 238, 58–70. [PubMed: 27448444]
108. Nehoff H, Parayath NN, Domanovitch L, Taurin S and Greish K (2014) Nanomedicine for drug targeting: Strategies beyond the enhanced permeability and retention effect. *Int. J. Nanomedicine* 9, 2539–2555. [PubMed: 24904213]
109. Golombek SK, May JN, Theek B, Appold L, Drude N, Kiessling F and Lammers T (2018) Tumor targeting via EPR: Strategies to enhance patient responses. *Adv. Drug Deliv. Rev* 130, 1–50. [PubMed: 30146082]
110. Jain RK and Stylianopoulos T (2010) Delivering nanomedicine to solid tumors. *Nat. Rev. Clin. Oncol* 7, 653–664. [PubMed: 20838415]
111. Jain RK (2012) Delivery of molecular and cellular medicine to solid tumors. *Adv. Drug Deliv. Rev* 46, 149–168.
112. Dewhirst MW and Secomb TW (2017) Transport of drugs from blood vessels to tumour tissue. *Nat. Rev. Cancer* 17, 738–750. [PubMed: 29123246]

113. Stapleton S, Milosevic M, Allen C, Zheng J, Dunne M, Yeung I and Jaffray DA (2013) A mathematical model of the enhanced permeability and retention effect for liposome transport in solid tumors. *PLoS One* 8, 1–10.
114. Goel S, Wong AHK and Jain RK (2012) Vascular normalization as a therapeutic strategy for malignant and nonmalignant disease. *Cold Spring Harb. Perspect. Med* 2, 1–24.
115. Jain RK, Tong RT and Munn LL (2007) Effect of vascular normalization by antiangiogenic therapy on interstitial hypertension, peritumor edema, and lymphatic metastasis: Insights from a mathematical model. *Cancer Res.* 67, 2729–2735. [PubMed: 17363594]
116. Fang H and DeClerck YA (2013) Targeting the tumor microenvironment: From understanding pathways to effective clinical trials. *Cancer Res.* 73, 4965–4977. [PubMed: 23913938]
117. Tsai M-J, Chang W-A, Huang M-S and Kuo P-L (2014) Tumor Microenvironment: A New Treatment Target for Cancer. *ISRN Biochem.* 2014, 1–8.
118. Gyenge EB, Forny P, Lüscher D, Laass A, Walt H and Maake C (2012) Effects of hypericin and a chlorin based photosensitizer alone or in combination in squamous cell carcinoma cells in the dark. *Photodiagnosis Photodyn. Ther* 9, 321–331. [PubMed: 23200013]
119. Shirata C, Kaneko J, Inagaki Y, Kokudo T, Sato M, Kiritani S, Akamatsu N, Arita J, Sakamoto Y, Hasegawa K and Kokudo N (2017) Near-infrared photothermal/photodynamic therapy with indocyanine green induces apoptosis of hepatocellular carcinoma cells through oxidative stress. *Sci. Rep* 7, 1–8. [PubMed: 28127051]
120. Obaid G, Huang H-C and Hasan T (2016) CHAPTER 8 Targeted Photodynamic Therapy—An Assimilation of Successes, Challenges and Future Directions In *Photodynamic Medicine: From Bench to Clinic*, pp. 137–160. The Royal Society of Chemistry.
121. Castano AP, Demidova TN and Hamblin MR (2004) Mechanisms in photodynamic therapy: Part one - Photosensitizers, photochemistry and cellular localization. *Photodiagnosis Photodyn. Ther* 1, 279–293. [PubMed: 25048432]
122. Lucky SS, Soo KC and Zhang Y (2015) Nanoparticles in photodynamic therapy. *Chem. Rev* 115, 1990–2042. [PubMed: 25602130]
123. Kessel D (2015) Apoptosis and associated phenomena as a determinants of the efficacy of photodynamic therapy. *Photochem. Photobiol. Sci* 14, 1397–1402. [PubMed: 25559971]
124. Li D, Li L, Li P, Li Y and Chen X (2015) Apoptosis of HeLa cells induced by a new targeting photosensitizer-based PDT via a mitochondrial pathway and ER stress. *Onco. Targets. Ther* 8, 703–711. [PubMed: 25897245]
125. Allison RR and Moghissi K (2013) Photodynamic Therapy (PDT): PDT Mechanisms. *Clin. Endosc* 46, 24–29. [PubMed: 23422955]
126. Kawczyk-Krupka A, Czuba Z, Szliszka E, Król W and Siero A (2011) The role of photosensitized macrophages in photodynamic therapy. *Oncol. Rep* 26, 275–280. [PubMed: 21503580]
127. Mroz P, Yaroslavsky A, Kharkwal GB and Hamblin MR (2011) Cell death pathways in photodynamic therapy of cancer. *Cancers (Basel)*. 3, 2516–2539. [PubMed: 23914299]
128. Kessel D and Reiners JJ (2017) Effects of Combined Lysosomal and Mitochondrial Photodamage in a Non Small-Cell Lung Cancer Cell Line: the Role of Paraptosis. *Photochem. Photobiol* 93, 1502–1508. [PubMed: 28696570]
129. Cincotta L, Szeto D, Lampros E, Hasan T and Cincotta AH (1996) Benzophenothiazine and benzoporphyrin derivative combination phototherapy effectively eradicates large murine sarcomas. *Photochem. Photobiol* 63, 229–237. [PubMed: 8657737]
130. Villanueva A, Stockert JC, Cañete M and Acedo P (2010) A new protocol in photodynamic therapy: Enhanced tumour cell death by combining two different photosensitizers. *Photochem. Photobiol. Sci* 9, 295–297. [PubMed: 20221454]
131. Acedo P, Stockert JC, Cañete M and Villanueva A (2014) Two combined photosensitizers: A goal for more effective photodynamic therapy of cancer. *Cell Death Dis.* 5, 1–12.
132. Kessel D and Reiners JJ (2014) Enhanced Efficacy of Photodynamic Therapy via a Sequential Targeting Protocol. *Photochem. Photobiol* 90, 889–895. [PubMed: 24617972]

133. Rizvi I, Obaid G, Bano S, Hasan T and Kessel D (2018) Photodynamic therapy: Promoting in vitro efficacy of photodynamic therapy by liposomal formulations of a photosensitizing agent. *Lasers Surg. Med* 50, 499–505. [PubMed: 29527710]
134. Rizvi I, Nath S, Obaid G, Ruhi MK, Moore K, Bano S, Kessel D and Hasan T (2019) A Combination of Visudyne and a Lipid-anchored Liposomal Formulation of Benzoporphyrin Derivative Enhances Photodynamic Therapy Efficacy in a 3D Model for Ovarian Cancer. *Photochem. Photobiol* 95, 419–429. [PubMed: 30499113]
135. Obaid G, Jin W, Bano S, Kessel D and Hasan T (2019) Nanolipid Formulations of Benzoporphyrin Derivative: Exploring the Dependence of Nanoconstruct Photophysics and Photochemistry on Their Therapeutic Index in Ovarian Cancer Cells. *Photochem. Photobiol* 95, 364–377. [PubMed: 30125366]
136. Inglut CT, Baglo Y, Liang BJ, Cheema Y, Stabile J, Woodworth GF and Huang H-C (2019) Systematic Evaluation of Light-Activatable Biohybrids for Anti-Glioma Photodynamic Therapy. *J. Clin. Med* 8, 1269.
137. Duska LR, Hamblin MR, Miller JL and Hasan T (1999) Combination Photoimmunotherapy and Cisplatin: Effects on Human Ovarian Cancer Ex Vivo. *JNCI J. Natl. Cancer Inst* 91, 1557–1563. [PubMed: 10491432]
138. Rizvi I, Celli JP, Evans CL, Abu-Yousif AO, Muzikansky A, Pogue BW, Finkelstein D and Hasan T (2010) Synergistic enhancement of carboplatin efficacy with photodynamic therapy in a three-dimensional model for micrometastatic ovarian cancer. *Cancer Res.* 70, 9319–9328. [PubMed: 21062986]
139. del Carmen MG, Rizvi I, Chang Y, Moor ACE, Oliva E, Sherwood M, Pogue B and Hasan T (2005) Synergism of epidermal growth factor receptor-targeted immunotherapy with photodynamic treatment of ovarian cancer in vivo. *J. Natl. Cancer Inst* 97, 1516–1524. [PubMed: 16234565]
140. Huang HC, Rizvi I, Liu J, Anbil S, Kalra A, Lee H, Baglo Y, Paz N, Hayden D, Pereira S, Pogue BW, Fitzgerald J and Hasan T (2018) Photodynamic priming mitigates chemotherapeutic selection pressures and improves drug delivery. *Cancer Res.* 78, 558–571. [PubMed: 29187403]
141. Spring BQ, Bryan Sears R, Zheng LZ, Mai Z, Watanabe R, Sherwood ME, Schoenfeld DA, Pogue BW, Pereira SP, Villa E and Hasan T (2016) A photoactivable multi-inhibitor nanoliposome for tumour control and simultaneous inhibition of treatment escape pathways. *Nat. Nanotechnol* 11, 378–387. [PubMed: 26780659]
142. Pigula M, Huang H-C, Mallidi S, Anbil S, Liu J, Mai Z and Hasan T (2019) Size-dependent Tumor Response to Photodynamic Therapy and Irinotecan Monotherapies Revealed by Longitudinal Ultrasound Monitoring in an Orthotopic Pancreatic Cancer Model. *Photochem. Photobiol* 95, 378–386. [PubMed: 30229942]
143. Huang HC, Mallidi S, Liu J, Chiang C. Te , Mai Z, Goldschmidt R, Ebrahim-Zadeh N, Rizvi I and Hasan T (2016) Photodynamic therapy synergizes with irinotecan to overcome compensatory mechanisms and improve treatment outcomes in pancreatic cancer. *Cancer Res.* 76, 1066–1077. [PubMed: 26719532]
144. van Straten D, Mashayekhi V, de Bruijn HS, Oliveira S and Robinson DJ (2017) Oncologic photodynamic therapy: Basic principles, current clinical status and future directions. *Cancers (Basel)*. 9, 1–54.
145. Solban N, Rizvi I and Hasan T (2006) Targeted photodynamic therapy. *Lasers Surg. Med* 38, 522–531. [PubMed: 16671102]
146. Wang H-W, Putt ME, Emanuele MJ, Shin DB, Glatstein E, Yodh AG and Busch TM (2004) Treatment-Induced Changes in Tumor Oxygenation Predict Photodynamic Therapy Outcome. *Cancer Res.* 64, 7553 LP–7561. [PubMed: 15492282]
147. Snyder JW, Greco WR, Bellnier DA, Vaughan L and Henderson BW (2003) Photodynamic Therapy: A Means to Enhanced Drug Delivery to Tumors. *Cancer Res.* 63, 8126–8131. [PubMed: 14678965]
148. Gil M, Bieniasz M, Seshadri M, Fisher D, Ciesielski MJ, Chen Y, Pandey RK and Kozbor D (2011) Photodynamic therapy augments the efficacy of oncolytic vaccinia virus against primary and metastatic tumours in mice. *Br. J. Cancer* 105, 1512–1521. [PubMed: 21989183]

149. Perentes JY, Wang Y, Wang X, Abdelnour E, Gonzalez M, Decosterd L, Wagnieres G, van den Bergh H, Peters S, Ris H-B and Krueger T (2014) Low-Dose Vascular Photodynamic Therapy Decreases Tumor Interstitial Fluid Pressure, which Promotes Liposomal Doxorubicin Distribution in a Murine Sarcoma Metastasis Model. *Transl. Oncol* 7, 393–399.
150. Lapík L and Schurz J (1991) Photochemical degradation of hyaluronic acid by singlet oxygen. *Colloid Polym. Sci* 269, 633–635.
151. Alageel SA, Arafat SN, Salvador-Culla B, Kolovou PE, Jahanseir K, Kozak A, Braithwaite GJC and Ciolino JB (2018) Corneal Cross-Linking with Verteporfin and Nonthermal Laser Therapy. *Cornea* 37, 362–368. [PubMed: 29176450]
152. Abbas S, Barbara R and Barbara A (2017) Water Soluble Tetrazolium Salt-11 as an Alternative to Riboflavin for Corneal Collagen Cross-linking for the Treatment of Keratoconus. *Int. J. Keratoconus Ectatic Corneal Dis* 6, 42–44.
153. Overhaus M, Heckenkamp J, Kossodo S, Leszczynski D and LaMuraglia GM (2000) Photodynamic therapy generates a matrix barrier to invasive vascular cell migration. *Circ. Res* 86, 334–340. [PubMed: 10679486]
154. Waterman PR, Overhaus M, Heckenkamp J, Nigri GR, Fungalo PFC, Landis ME, Kossodo SC and LaMuraglia GM (2004) Mechanisms of Reduced Human Vascular Cell Migration After Photodynamic Therapy. *Photochem. Photobiol* 75, 46–50.
155. Tanaka H, Okada T, Konishi H and Tsuji T (1993) The effect of reactive oxygen species on the biosynthesis of collagen and glycosaminoglycans in cultured human dermal fibroblasts. *Arch. Dermatol. Res* 285, 352–355. [PubMed: 8215584]
156. Karrer S, Bosserhoff AK, Weiderer P, Landthaler M and Szeimies RM (2003) Influence of 5-aminolevulinic acid and red light on collagen metabolism of human dermal fibroblasts. *J. Invest. Dermatol* 120, 325–331. [PubMed: 12542540]
157. Gomer CJ, Ferrario A, Luna M, Rucker N and Wong S (2006) Photodynamic therapy: Combined modality approaches targeting the tumor microenvironment. *Lasers Surg. Med* 38, 516–521. [PubMed: 16607618]
158. Fleming JM, Yeyeodu ST, McLaughlin A, Schuman D and Taylor DK (2018) In Situ Drug Delivery to Breast Cancer-Associated Extracellular Matrix. *ACS Chem. Biol* 13, 2825–2840. [PubMed: 30183254]
159. Özdemir BC, Pentcheva-Hoang T, Carstens JL, Zheng X, Wu C-C, Simpson TR, Laklai H, Sugimoto H, Kahlert C, Novitskiy SV, De Jesus-Acosta A, Sharma P, Heidari P, Mahmood U, Chin L, Moses HL, Weaver VM, Maitra A, Allison JP, LeBleu VS and Kalluri R (2014) Depletion of carcinoma-associated fibroblasts and fibrosis induces immunosuppression and accelerates pancreas cancer with reduced survival. *Cancer Cell* 25, 719–734. [PubMed: 24856586]
160. Malham GM, Thomsen RJ, Finlay GJ, B. CB (1996) Subcellular distribution and photocytotoxicity of aluminium phthalocyanines and haematoporphyrin derivative in cultured human meningioma cells. *Br. J. Neurosurg* 10, 51–57. [PubMed: 8672259]
161. Miller W, Walsh AW, Kramer M, Hasan T, Michaud N, Flotte TJ, Haimovici R and Gragoudas ES (1995) Photodynamic Therapy of Experimental Choroidal Neovascularization Using Lipoprotein-Delivered Benzoporphyrin. *Arch. Dermatol. Res* 113, 810–818.
162. Runnels JM, Chen N, Ortel B, Kato D and Hasan T (1999) BPD-MA-mediated photosensitisation in vitro and in vivo: Cellular adhesion and  $\beta$ 1 integrin expression in ovarian cancer cells. *Br. J. Cancer* 80, 946–953. [PubMed: 10362101]
163. Kawczyk-Krupka A, Wawrzyniec K, Musiol SK, Potempa M, Bugaj AM and Siero A (2015) Treatment of localized prostate cancer using WST-09 and WST-11 mediated vascular targeted photodynamic therapy-A review. *Photodiagnosis Photodyn. Ther* 12, 567–574. [PubMed: 26467273]
164. Hsieh YJ, Wu CC, Chang CJ and Yu JS (2003) Subcellular localization of photofrin® determines the death phenotype of human epidermoid carcinoma A431 cells triggered by photodynamic therapy: When plasma membranes are the main targets. *J. Cell. Physiol* 194, 363–375. [PubMed: 12548556]

165. Marchal S, François A, Dumas D, Guillemin F and Bezdetsnaya L (2007) Relationship between subcellular localisation of Foscan® and caspase activation in photosensitised MCF-7 cells. *Br. J. Cancer* 96, 944–951. [PubMed: 17325708]
166. Teiten MH, Bezdetsnaya L, Morlière P, Santus R and Guillemin F (2003) Endoplasmic reticulum and Golgi apparatus are the preferential sites of Foscan® localisation in cultured tumour cells. *Br. J. Cancer* 88, 146–152. [PubMed: 12556974]
167. Tynga IM, Houeild NN and Abrahamse H (2013) The primary subcellular localization of Zinc phthalocyanine and its cellular impact on viability, proliferation and structure of breast cancer cells (MCF-7). *J. Photochem. Photobiol. B Biol* 120, 171–176.
168. Kessel D, Woodburn K, Gomer CJ, Jagerovic N and Smith KM (1995) Photosensitization with derivatives of chlorin p6. *J. Photochem. Photobiol. B Biol* 28, 13–18.
169. Gaullier J-M, Gèze M, Santus R, Melo T. S. e., Mazière J-C, Bazin M, Morlière P and Dubertret L (1995) Subcellular Localization of and Photosensitization by Protoporphyrin IX in Human Keratinocytes and Fibroblasts cultivated with 5-Aminolevulinic Acid. *Photochem. Photobiol* 62, 114–122. [PubMed: 7638255]
170. Shulok JR, Wade MH and Lin C-W (1990) Subcellular localization of hematoporphyrin derivative in bladder tumor cells in culture. *Photochem. Photobiol* 51, 451–457. [PubMed: 2140450]
171. Shemin D and Rittenberg D (1945) The utilization of glycine for the synthesis of a porphyrin. *J. Biol. Chem* 159, 567–568.
172. Shemin D and Russell C (1953) Aminolevulinic acid, its role in the biosynthesis of porphyrins and purines. *J. Am. Chem. Soc* 75, 4873–4873.
173. Radin N, Rittenberg D and Shemin D (1950) The role of acetic acid in the biosynthesis of heme. *J. Biol. Chem* 184, 755–767. [PubMed: 15428460]
174. Muir HM and Neuberger A (1950) The biogenesis of porphyrins. 2. The origin of the methyne carbon atoms. *Biochem. J* 47, 97–104. [PubMed: 14791314]
175. Gibson KD, Laver WG and Neuberger A (1958) Initial stages in the biosynthesis of porphyrins. 2. The formation of delta-aminolaevulinic acid from glycine and succinyl-coenzyme A by particles from chicken erythrocytes. *Biochem. J* 70, 71–81. [PubMed: 13584304]
176. Kikuchi G, Kumar A, Talmage P and Shemin D (1958) The enzymatic synthesis of delta-aminolevulinic acid. *J. Biol. Chem* 233, 1214–1219. [PubMed: 13598764]
177. Shemin D and Kumin S (1952) The mechanism of porphyrin formation; the formation of a succinyl intermediate from succinate. *J. Biol. Chem* 198, 827–837. [PubMed: 12999801]
178. Yamamoto M, Fujita H, Katase N, Inoue K, Nagatsuka H, Utsumi K, Sasaki J and Ohuchi H (2013) Improvement of the efficacy of 5-aminolevulinic acid-mediated photodynamic treatment in human oral squamous cell carcinoma hsc-4. *Acta Med. Okayama* 67, 153–164. [PubMed: 23804138]
179. Kobuchi H, Moriya K, Ogino T, Fujita H, Inoue K, Shuin T, Yasuda T, Utsumi K and Utsumi T (2012) Mitochondrial Localization of ABC Transporter ABCG2 and Its Function in 5-Aminolevulinic Acid-Mediated Protoporphyrin IX Accumulation. *PLoS One* 7, 1–14.
180. Hadjipanayis CG and Stummer W (2019) 5-ALA and FDA approval for glioma surgery. *J. Neurooncol* 141, 479–486. [PubMed: 30644008]
181. Dirschka T, Radny P, Dominicus R, Mensing H, Brüning H, Jenne L, Karl L, Sebastian M, Oster-Schmidt C, Klövekorn W, Reinhold U, Tanner M, Gröne D, Deichmann M, Simon M, Hübinger F, Hofbauer G, Krähn-Senftleben G, Borrosch F, Reich K, Berking C, Wolf P, Lehmann P, Moers-Carpi M, Hönigsmann H, Wernicke-Panten K, Helwig C, Foguet M, Schmitz B, Lübbert H and Szeimies RM (2012) Photodynamic therapy with BF-200 ALA for the treatment of actinic keratosis: Results of a multicentre, randomized, observer-blind phase III study in comparison with a registered methyl-5-aminolaevulinic acid cream and placebo. *Br. J. Dermatol* 166, 137–146. [PubMed: 21910711]
182. Dirschka T, Radny P, Dominicus R, Mensing H, Brüning H, Jenne L, Karl L, Sebastian M, Oster-Schmidt C, Klövekorn W, Reinhold U, Tanner M, Gröne D, Deichmann M, Simon M, Hübinger F, Hofbauer G, Krähn-Senftleben G, Borrosch F, Reich K, Berking C, Wolf P, Lehmann P, Moers-Carpi M, Hönigsmann H, Wernicke-Panten K, Hahn S, Pabst G, Voss D, Foguet M, Schmitz B, Lübbert H and Szeimies RM (2013) Long-term (6 and 12 months) follow-up of two

- prospective, randomized, controlled phase III trials of photodynamic therapy with BF-200 ALA and methyl aminolaevulinate for the treatment of actinic keratosis. *Br. J. Dermatol* 168, 825–836. [PubMed: 23252768]
183. DUSA Pharmaceuticals I (1999) LEVULAN ® KERASTICK TM (aminolevulinic acid HCl) for Topical Solution, 20% For Topical Use Only Not for Ophthalmic Use. Cranston, RI.
184. Wachowska M, Muchowicz A, Firczuk M, Gabrysiak M, Winiarska M, Wa czyk M, Bojarczuk K and Golab J (2011) Aminolevulinic acid (ala) as a prodrug in photodynamic therapy of cancer. *Molecules* 16, 4140–4164.
185. Malik Z and Djaldetti M (1979) 5-aminolevulinic acid stimulation of porphyrin and hemoglobin synthesis by uninduced friend erythroleukemic cells. *Cell Differ.* 8, 223–233. [PubMed: 288514]
186. Kennedy JC, Pottier RH and Pross DC (1990) Photodynamic therapy with endogenous protoporphyrin. IX: Basic principles and present clinical experience. *J. Photochem. Photobiol. B Biol* 6, 143–148.
187. Pottier R, Krammer B, Stepp H and Baumgartner R (2006) Photodynamic Therapy with ALA: A Clinical Handbook 6th ed The Royal Society of Chemistry, Cambridge, UK.
188. Kennedy JC and Pottier RH (1992) New trends in photobiology. Endogenous protoporphyrin IX, a clinically useful photosensitizer for photodynamic therapy. *J. Photochem. Photobiol. B Biol* 14, 275–292.
189. K. JC and P. RH (1992) Endogenous protoporphyrin IX, a clinically useful photosensitizer for photodynamic therapy. *J. Photochem. Photobiol. B Biol* 14, 275–292.
190. Gad F, Viau G, Boushira M, Bertrand R and Bissonnette R (2001) Photodynamic therapy with 5-aminolevulinic acid induces apoptosis and caspase activation in malignant T cells. *J. Cutan. Med. Surg* 5, 8–13. [PubMed: 11281435]
191. Anand S, Wilson C, Hasan T and Maytin EV (2011) Vitamin D3 enhances the apoptotic response of epithelial tumors to aminolevulinic acid-based photodynamic therapy. *Cancer Res.* 71, 6040–6050. [PubMed: 21807844]
192. Rollakanti KR, Anand S and Maytin EV (2015) Vitamin D enhances the efficacy of photodynamic therapy in a murine model of breast cancer. *Cancer Med.* 4, 633–642. [PubMed: 25712788]
193. Maytin EV, Anand S, Wilson C and Iyer K (2011) 5-Fluorouracil as an enhancer of aminolevulinic acid-based photodynamic therapy for skin cancer: New use for a venerable agent? In *Optical Methods for Tumor Treatment and Detection: Mechanisms and Techniques in Photodynamic Therapy XX*.
194. Tahmasebi H, Khoshgard K, Sazgarnia A, Mostafaie A and Eivazi MT (2016) Enhancing the efficiency of 5-aminolevulinic acid-mediated photodynamic therapy using 5-fluorouracil on human melanoma cells. *Photodiagnosis Photodyn. Ther* 13, 297–302. [PubMed: 26321747]
195. Benito-Miguel M, Blanco MD and Gómez C (2015) Assessment of sequential combination of 5-fluorouracil-loaded-chitosan-nanoparticles and ALA-photodynamic therapy on HeLa cell line. *Photodiagnosis Photodyn. Ther* 12, 466–475. [PubMed: 25976508]
196. Maytin EV, Anand S, Riha M, Lohser S, Tellez A, Ishak R, Karpinski L, Sot J, Hu B, Denisjuk A, Davis SC, Kyei A and Vidimos A (2018) 5-fluorouracil enhances protoporphyrin IX accumulation and lesion clearance during photodynamic therapy of actinic keratoses: A mechanism-based clinical trial. *Clin. Cancer Res* 24, 3026–3035. [PubMed: 29593028]
197. Salim A, Leman JA, McColl JH, Chapman R and Morton CA (2003) Randomized comparison of photodynamic therapy with topical 5-fluorouracil in Bowen’s disease. *Br. J. Dermatol* 148, 539–543. [PubMed: 12653747]
198. Blake E and Curnow A (2010) The hydroxypyridinone iron chelator CP94 can enhance PpIX-induced PDT of cultured human glioma cells. *Photochem. Photobiol* 86, 1154–1160. [PubMed: 20573043]
199. Hanania J and Malik Z (1992) The effect of EDTA and serum on endogenous porphyrin accumulation and photodynamic sensitization of human K562 leukemic cells. *Cancer Lett.* 65, 127–131. [PubMed: 1511416]
200. Pye A, Campbell S and Curnow A (2008) Enhancement of methyl-aminolevulinic acid photodynamic therapy by iron chelation with CP94: An in vitro investigation and clinical dose-escalating safety

- study for the treatment of nodular basal cell carcinoma. *J. Cancer Res. Clin. Oncol* 134, 841–849. [PubMed: 18239941]
201. Campbell SM, Morton CA, Alyahya R, Horton S, Pye A and Curnow A (2008) Clinical investigation of the novel iron-chelating agent, CP94, to enhance topical photodynamic therapy of nodular basal cell carcinoma. *Br. J. Dermatol* 159, 387–393. [PubMed: 18544077]
202. Pye A and Curnow A (2007) Direct Comparison of  $\delta$ -Aminolevulinic Acid and Methyl-Aminolevulinate-Derived Protoporphyrin IX Accumulations Potentiated by Desferrioxamine or the Novel Hydroxypyridinone Iron Chelator CP94 in Cultured Human Cells. *Photochem. Photobiol* 83, 766–773. [PubMed: 17576385]
203. Anand S, Rollakanti KR, Horst RL, Hasan T and Maytin EV (2014) Combination of Oral Vitamin D3 with Photodynamic Therapy Enhances Tumor Cell Death in a Murine Model of Cutaneous Squamous Cell Carcinoma. *Photochem. Photobiol* 90, 1126–1135. [PubMed: 24807677]
204. Berg K, Anholt H, Bech and Moan J (1996) The influence of iron chelators on the accumulation of protoporphyrin IX in 5-aminolaevulinic acid-treated cells. *Br. J. Cancer* 74, 688–697. [PubMed: 8795569]
205. Bech, Phillips D, Moan J and MacRobert AJ (1997) A hydroxypyridinone (CP94) enhances protoporphyrin IX formation in 5-aminolaevulinic acid treated cells. *J. Photochem. Photobiol. B Biol* 41, 136–144.
206. Curnow A, MacRobert AJ and Bown SG (2006) Comparing and combining light dose fractionation and iron chelation to enhance experimental photodynamic therapy with aminolevulinic acid. *Lasers Surg. Med* 38, 325–331. [PubMed: 16596660]
207. Chang SC, MacRobert AJ, Porter JB and Bown SG (1997) The efficacy of an iron chelator (CP94) in increasing cellular protoporphyrin IX following intravesical 5-aminolaevulinic acid administration: An in vivo study. *J. Photochem. Photobiol. B Biol* 38, 114–122.
208. Casas A, Del C Batlle AM, Butler AR, Robertson D, Brown EH, MacRobert A and Riley PA (1999) Comparative effect of ALA derivatives on protoporphyrin IX production in human and rat skin organ cultures. *Br. J. Cancer* 80, 1525–1532. [PubMed: 10408393]
209. Choudry K, Brooke RCC, Farrar W and Rhodes LE (2003) The effect of an iron chelating agent on protoporphyrin IX levels and phototoxicity in topical 5-aminolaevulinic acid photodynamic therapy. *Br. J. Dermatol* 149, 124–130. [PubMed: 12890205]
210. Inoue K, Karashima T, Kamada M, Shuin T, Kurabayashi A, Furihata M, Fujita H, Utsumi K and Sasaki J (2009) Regulation of 5-aminolevulinic acid-mediated protoporphyrin IX accumulation in human urothelial carcinomas. *Pathobiology* 76, 303–314. [PubMed: 19955842]
211. Ortel B, Sharlin D, O'Donnell D, Sinha AK, Maytin EV and Hasan T (2002) Differentiation enhances aminolevulinic acid-dependent photodynamic treatment of LNCaP prostate cancer cells. *Br. J. Cancer* 87, 1321–1327. [PubMed: 12439724]
212. Maytin EV, Honari G, Khachemoune A, Taylor CR, Ortel B, Pogue BW, Szynger-Taub N and Hasan T (2012) Vitamin D Combined with Aminolevulinic Acid (ALA)-Mediated Photodynamic Therapy (PDT) for Human Psoriasis: A Proof-of-Principle Study. *Isr. J. Chem* 59, 767–775.
213. Seo JW and Song KH (2018) Topical calcipotriol before ablative fractional laser-assisted photodynamic therapy enhances treatment outcomes for actinic keratosis in Fitzpatrick grades III–V skin: A prospective randomized clinical trial. *J. Am. Acad. Dermatol* 78, 795–797. [PubMed: 29138062]
214. Momma T, Hamblin MR and Hasan T (1997) Hormonal modulation of the accumulation of 5-aminolevulinic acid-induced protoporphyrin and phototoxicity in prostate cancer cells. *Int. J. Cancer* 72, 1062–1069. [PubMed: 9378541]
215. Sinha AK, Anand S, Ortel BJ, Chang Y, Mai Z, Hasan T and Maytin EV (2006) Methotrexate used in combination with aminolaevulinic acid for photodynamic killing of prostate cancer cells. *Br. J. Cancer* 95, 485–495. [PubMed: 16868543]
216. Anand S, Honari G, Hasan T, Elson P and Maytin EV (2009) Low-dose methotrexate enhances aminolevulinic acid-based photodynamic therapy in skin carcinoma cells in vitro and in vivo. *Clin. Cancer Res.* 15, 3333–3343. [PubMed: 19447864]

217. Yang DF, Lee JW, Chen HM and Hsu YC (2014) Topical methotrexate pretreatment enhances the therapeutic effect of topical 5-aminolevulinic acid-mediated photodynamic therapy on hamster buccal pouch precancers. *J. Formos. Med. Assoc* 113, 591–599. [PubMed: 24811932]
218. Juzeniene A, Juzenas P, Bronshtein I, Vorobey A and Moan J (2006) The influence of temperature on photodynamic cell killing in vitro with 5-aminolevulinic acid. *J. Photochem. Photobiol. B Biol* 84, 161–166.
219. Juzeniene A, Juzenas P, Iani V and Moan J (2004) Topical Application of 5-Aminolevulinic Acid and its Methylene, Hexylester and Octylester Derivatives: Considerations for Dosimetry in Mouse Skin Model. *Photochem. Photobiol* 76, 329–334.
220. Piot B, Rousset N, Lenz P, Eléouet S, Carré J, Vonarx V, Bourré L and Patrice T (2001) Enhancement of delta aminolevulinic acid-photodynamic therapy in vivo by decreasing tumor pH with glucose and amiloride. *Laryngoscope* 111, 2205–2213. [PubMed: 11802027]
221. Bech, Berg K and Moan J (1997) The pH dependency of protoporphyrin IX formation in cells incubated with 5-aminolevulinic acid. *Cancer Lett.* 113, 25–29. [PubMed: 9065797]
222. Wyld L, Reed MWR and Brown NJ (1998) The influence of hypoxia and pH on aminolaevulinic acid-induced photodynamic therapy in bladder cancer cells in vitro. *Br. J. Cancer* 77, 1621–1627. [PubMed: 9635837]
223. Uehlinger P, Zellweger M, Wagnières G, Juillerat-Jeanneret L, Van Den Bergh H and Lange N (2000) 5-Aminolevulinic acid and its derivatives: Physical chemical properties and protoporphyrin IX formation in cultured cells. *J. Photochem. Photobiol. B Biol* 54, 72–80.
224. Ulrich TA, de Juan Pardo EM and Kumar S (2009) The mechanical rigidity of the extracellular matrix regulates the structure, motility, and proliferation of glioma cells. *Cancer Res.* 69, 4167–4174. [PubMed: 19435897]
225. Murphy MC, Huston J, Jack CR, Glaser KJ, Manduca A, Felmlee JP and Ehman RL (2011) Decreased brain stiffness in Alzheimer's disease determined by magnetic resonance elastography. *J. Magn. Reson. Imaging* 34, 494–498. [PubMed: 21751286]
226. Fisher CJ, Niu CJ, Lai B, Chen Y, Kuta V and Lilge LD (2013) Modulation of PPIX synthesis and accumulation in various normal and glioma cell lines by modification of the cellular signaling and temperature. *Lasers Surg. Med* 45, 460–468. [PubMed: 24037824]
227. Wang M, Zhao J, Zhang L, Wei F, Lian Y, Wu Y, Gong Z, Zhang S, Zhou J, Cao K, Li X, Xiong W, Li G, Zeng Z and Guo C (2017) Role of tumor microenvironment in tumorigenesis. *J. Cancer* 8, 761–773. [PubMed: 28382138]
228. Greish K (2010) Enhanced permeability and retention (EPR) effect for anticancer nanomedicine drug targeting. *Methods Mol. Biol* 624, 25–37. [PubMed: 20217587]
229. Rosenblum D, Joshi N, Tao W, Karp JM and Peer D (2018) Progress and challenges towards targeted delivery of cancer therapeutics. *Nat. Commun* 9, 1–12. [PubMed: 29317637]
230. Thews O and Riemann A (2019) Tumor pH and metastasis: a malignant process beyond hypoxia. *Cancer Metastasis Rev.* 38, 113–129. [PubMed: 30607627]
231. Kato Y, Ozawa S, Miyamoto C, Maehata Y, Suzuki A, Maeda T and Baba Y (2013) Acidic extracellular microenvironment and cancer. *Cancer Cell Int.* 13(1), 1–8. [PubMed: 23305405]
232. Liberti MV and Locasale JW (2016) The Warburg Effect: How Does it Benefit Cancer Cells? *Trends Biochem. Sci* 41, 211–218. [PubMed: 26778478]
233. Matsumura Y and Maeda H (1986) A New Concept for Macromolecular Therapeutics in Cancer Chemotherapy: Mechanism of Tumorotropic Accumulation of Proteins and the Antitumor Agent Smancs. *Cancer Res.* 46, 6387–6392. [PubMed: 2946403]
234. Prabhakar U, Maeda H, Jain R, Sevick-Muraca EM, Zamboni W, Farokhzad OC, Barry ST, Gabizon A, Grodzinski P and Blakey DC (2013) Challenges and key considerations of the enhanced permeability and retention effect for nanomedicine drug delivery in oncology. *Cancer Res.* 73, 2412–2417. [PubMed: 23423979]
235. Torchilin V (2011) Tumor delivery of macromolecular drugs based on the EPR effect. *Adv. Drug Deliv. Rev* 63, 131–135. [PubMed: 20304019]
236. Lim CK, Heo J, Shin S, Jeong K, Seo YH, Jang WD, Park CR, Park SY, Kim S and Kwon IC (2013) Nanophotosensitizers toward advanced photodynamic therapy of Cancer. *Cancer Lett.* 334, 176–187. [PubMed: 23017942]

237. Weijer R, Broekgaarden M, Kos M, van Vught R, Rauws EAJ, Breukink E, van Gulik TM, Storm G and Heger M (2015) Enhancing photodynamic therapy of refractory solid cancers: Combining second-generation photosensitizers with multi-targeted liposomal delivery. *J. Photochem. Photobiol. C Photochem. Rev* 23, 103–131.
238. Kim J, Santos OA and Park JH (2014) Selective photosensitizer delivery into plasma membrane for effective photodynamic therapy. *J. Control. Release* 191, 98–104. [PubMed: 24892975]
239. Huang H-C, Mallidi S, Obaid G, Sears B, Tangutoori S and Hasan T (2015) 23 - Advancing photodynamic therapy with biochemically tuned liposomal nanotechnologies In *Applications of Nanoscience in Photomedicine* (Edited by Hamblin MR and Avci, P. B. T.-A. of N. in P.), pp. 487–510. Chandos Publishing, Oxford.
240. Baglo Y, Liang BJ, Robey RW, Ambudkar SV, Gottesman MM and Huang H-C (2019) Porphyrin-lipid assemblies and nanovesicles overcome ABC transporter-mediated photodynamic therapy resistance in cancer cells. *Cancer Lett.* 457, 110–118. [PubMed: 31071369]
241. Huynh E and Zheng G (2014) Porphysome nanotechnology: A paradigm shift in lipid-based supramolecular structures. *Nano Today* 9, 212–222.
242. Hsu CY, Chen CW, Yu HP, Lin YF and Lai PS (2013) Bioluminescence resonance energy transfer using luciferase-immobilized quantum dots for self-illuminated photodynamic therapy. *Biomaterials* 34, 1204–1212. [PubMed: 23069718]
243. Shao L, Gao Y and Yan F (2011) Semiconductor quantum dots for Biomedical applications. *Sensors* 11, 11736–11751. [PubMed: 22247690]
244. Lee KL, Carpenter BL, Wen AM, Ghiladi RA and Steinmetz NF (2016) High Aspect Ratio Nanotubes Formed by Tobacco Mosaic Virus for Delivery of Photodynamic Agents Targeting Melanoma. *ACS Biomater. Sci. Eng* 2, 838–844. [PubMed: 28713855]
245. Gandra N, Abbineni G, Qu X, Huai Y, Wang L and Mao C (2013) Bacteriophage bionanowire as a carrier for both cancer-targeting peptides and photosensitizers and its use in selective cancer cell killing by photodynamic therapy. *Small* 9, 215–221. [PubMed: 23047655]
246. Stephanopoulos N, Tong GJ, Hsiao SC and Francis MB (2010) Dual-surface modified virus capsids for targeted delivery of photodynamic agents to cancer cells. *ACS Nano* 4, 6014–6020. [PubMed: 20863095]
247. Rhee JK, Baksh M, Nycholat C, Paulson JC, Kitagishi H and Finn MG (2012) Glycan-targeted virus-like nanoparticles for photodynamic therapy. *Biomacromolecules* 13, 2333–2338. [PubMed: 22827531]
248. Bae BC and Na K (2012) Development of polymeric cargo for delivery of photosensitizer in photodynamic therapy. *Int. J. Photoenergy* 2012, 1–14.
249. Yang G, Gong H, Qian X, Tan P, Li Z, Liu T, Liu J, Li Y and Liu Z (2015) Mesoporous silica nanorods intrinsically doped with photosensitizers as a multifunctional drug carrier for combination therapy of cancer. *Nano Res.* 8, 751–764.
250. Bharathiraja S, Moorthy MS, Manivasagan P, Seo H, Lee KD and Oh J (2017) Chlorin e6 conjugated silica nanoparticles for targeted and effective photodynamic therapy. *Photodiagnosis Photodyn. Ther* 19, 212–220. [PubMed: 28583295]
251. Sun J, Kormakov S, Liu Y, Huang Y, Wu D and Yang Z (2018) Recent progress in metal-based nanoparticles mediated photodynamic therapy. *Molecules* 23, 1–23.
252. Lee DJ, Park SY, Oh YT, Oh NM, Oh KT, Youn YS and Lee ES (2011) Preparation of chlorine e6-conjugated single-wall carbon nanotube for photodynamic therapy. *Macromol. Res* 19, 848–852.
253. Huang P, Wang S, Wang X, Shen G, Lin J, Wang Z, Guo S, Cui D, Yang M and Chen X (2015) Surface functionalization of chemically reduced graphene oxide for targeted photodynamic therapy. *J. Biomed. Nanotechnol* 11, 117–125. [PubMed: 26301305]
254. Huang H and Hasan T (2014) The “ Nano ” World in Photodynamic Therapy. *Austin J Nanomed Nanotechnol* 2, 2–5.
255. Yin R, Wang M, Huang Y-Y, Huang H-C, Avci P, Chiang LY and Hamblin MR (2014) Photodynamic therapy with decacationic [60]fullerene monoadducts: effect of a light absorbing electron-donor antenna and micellar formulation. *Nanomedicine* 10, 795–808. [PubMed: 24333585]

256. Obaid G, Broekgaarden M, Bulin A-L, Huang H-C, Kuriakose J, Liu J and Hasan T (2016) Photonanomedicine: a convergence of photodynamic therapy and nanotechnology. *Nanoscale* 8, 12471–12503. [PubMed: 27328309]
257. Shi J, Kantoff PW, Wooster R and Farokhzad OC (2017) Cancer nanomedicine: Progress, challenges and opportunities. *Nat. Rev. Cancer* 17, 20–37. [PubMed: 27834398]
258. Miller MA, Arlauckas S and Weissleder R (2017) Prediction of Anti-cancer Nanotherapy Efficacy by Imaging. *Nanotheranostics* 1, 296–312. [PubMed: 29071194]
259. Miller MA, Gadde S, Pfirschke C, Engblom C, Sprachman MM, Kohler RH, Yang KS, Laughney AM, Wojtkiewicz G, Kamaly N, Bhonagiri S, Pittet MJ, Farokhzad OC and Weissleder R (2015) Predicting therapeutic nanomedicine efficacy using a companion magnetic resonance imaging nanoparticle. *Sci. Transl. Med* 7, 1–21.
260. Maeda H (2015) Toward a full understanding of the EPR effect in primary and metastatic tumors as well as issues related to its heterogeneity. *Adv. Drug Deliv. Rev* 91, 3–6. [PubMed: 25579058]
261. Rajora AK, Ravishankar D, Osborn HMI and Greco F (2014) Impact of the enhanced permeability and retention (EPR) effect and cathepsins levels on the activity of polymer-drug conjugates. *Polymers (Basel)*. 6, 2186–2220.
262. Chaffer CL and Weinberg RA (2011) A perspective on cancer cell metastasis. *Science (80-. )*. 331, 1559–1564.
263. Nichols JW and Bae YH (2014) EPR: Evidence and fallacy. *J. Control. Release* 190, 451–464. [PubMed: 24794900]
264. Chen B, Pogue BW, Luna JM, Hardman RL, Hoopes PJ and Hasan T (2006) Tumor vascular permeabilization by vascular-targeting photosensitization: Effects, mechanism, and therapeutic implications. *Clin. Cancer Res* 12, 917–923. [PubMed: 16467106]
265. Chen B, Pogue BW, Hoopes PJ and Hasan T (2005) Combining vascular and cellular targeting regimens enhances the efficacy of photodynamic therapy. *Int. J. Radiat. Oncol. Biol. Phys* 61, 1216–1226. [PubMed: 15752904]
266. Gao W, Wang Z, Lv L, Yin D, Chen D, Han Z, Ma Y, Zhang M, Yang M and Gu Y (2016) Photodynamic therapy induced enhancement of tumor vasculature permeability using an upconversion nanoconstruct for improved intratumoral nanoparticle delivery in deep tissues. *Theranostics* 6, 1131–1144. [PubMed: 27279907]
267. Zhen Z, Tang W, Chuang YJ, Todd T, Zhang W, Lin X, Niu G, Liu G, Wang L, Pan Z, Chen X and Xie J (2014) Tumor vasculature targeted photodynamic therapy for enhanced delivery of nanoparticles. *ACS Nano* 8, 6004–6013. [PubMed: 24806291]
268. Sano K, Nakajima T, Choyke PL and Kobayashi H (2013) Markedly enhanced permeability and retention effects induced by photo-immunotherapy of tumors. *ACS Nano* 7, 717–724. [PubMed: 23214407]
269. Kobayashi H and Choyke PL (2016) Super enhanced permeability and retention (SUPR) effects in tumors following near infrared photoimmunotherapy. *Nanoscale* 8, 12504–12509. [PubMed: 26443992]
270. Leunig M, Goetz AE, Gamarra F, Zetterer G, Messmer K and Jaim RK (1994) Photodynamic therapy-induced alterations in interstitial fluid pressure, volume and water content of an amelanotic melanoma in the hamster. *Br. J. Cancer* 69, 101–103. [PubMed: 8286189]
271. Cavin S, Riedel T, Roskopfova P, Gonzalez M, Baldini G, Zellweger M, Wagnières G, Dyson PJ, Ris HB, Krueger T and Perentes JY (2019) Vascular-targeted low dose photodynamic therapy stabilizes tumor vessels by modulating pericyte contractility. *Lasers Surg. Med* 51, 550–561. [PubMed: 30779366]
272. Fingar VH, Kik PK, Haydon PS, Cerrito PB, Tseng M, Abang E and Wieman TJ (1999) Analysis of acute vascular damage after photodynamic therapy using benzoporphyrin derivative (BPD). *Br. J. Cancer* 79, 1702–1708. [PubMed: 10206280]
273. Engbrecht BW, Menon C, Kachur AV, Hahn SM and Fraker DL (1999) Photofrin-mediated photodynamic therapy induces vascular occlusion and apoptosis in a human sarcoma xenograft model. *Cancer Res.* 59, 4334–4342. [PubMed: 10485481]

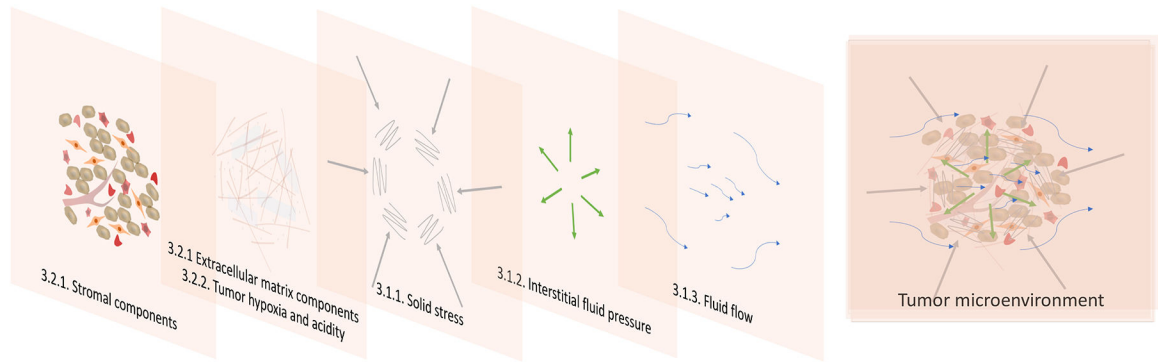
274. Madar-Balakisri N, Tempel-Brami C, Kalchenko V, Brenner O, Varon D, Scherz A and Salomon Y (2010) Permanent occlusion of feeding arteries and draining veins in solid mouse tumors by vascular Targeted Photodynamic Therapy (VTP) with tookad. *PLoS One* 5, 1–10.
275. Buzzá HH, de Freitas LCF, Moriyama LT, Rosa RGT, Bagnato VS and Kurachi C (2019) Vascular effects of photodynamic therapy with curcumin in a chorioallantoic membrane model. *Int. J. Mol. Sci* 20, 1–12.
276. Bugaj AM (2016) Vascular targeted photochemotherapy using padoporphin and padeliporphin as a method of the focal treatment of localised prostate cancer - clinician's insight. *World J. Methodol* 6, 65–76. [PubMed: 27019798]
277. Zilberstein J, Schreiber S, Bloemers MCWM, Bendel P, Neeman M, Schechtman E, Kohen F, Scherz A and Salomon Y (2001) Antivascular Treatment of Solid Melanoma Tumors with Bacteriochlorophyll–serine-based Photodynamic Therapy. *Photochem. Photobiol* 73, 257–266. [PubMed: 11281022]
278. Azzouzi AR, Barret E, Bennet J, Moore C, Taneja S, Muir G, Villers A, Coleman J, Allen C, Scherz A and Emberton M (2015) TOOKAD® Soluble focal therapy: pooled analysis of three phase II studies assessing the minimally invasive ablation of localized prostate cancer. *World J. Urol* 33, 945–953. [PubMed: 25712310]
279. Eggener SE and Coleman JA (2008) Focal treatment of prostate cancer with vascular-targeted photodynamic therapy. *ScientificWorldJournal*. 8, 963–973. [PubMed: 18836668]
280. Trachtenberg J, Weersink RA, Davidson SRH, Haider MA, Bogaards A, Gertner MR, Evans A, Scherz A, Savard J, Chin JL, Wilson BC and Elhilali M (2008) Vascular-targeted photodynamic therapy (padoporphin, WST09) for recurrent prostate cancer after failure of external beam radiotherapy: A study of escalating light doses. *BJU Int.* 102, 556–562. [PubMed: 18494829]
281. Azzouzi AR, Vincendeau S, Barret E, Cicco A, Kleinclauss F, van der Poel HG, Stief CG, Rassweiler J, Salomon G, Solsona E, Alcaraz A, Tammela TT, Rosario DJ, Gomez-Veiga F, Ahlgren G, Benzaghoul F, Gaillac B, Amzal B, Debruyne FMJ, Fromont G, Gratzke C and Emberton M (2017) Padeliporphin vascular-targeted photodynamic therapy versus active surveillance in men with low-risk prostate cancer (CLIN1001 PCM301): an open-label, phase 3, randomised controlled trial. *Lancet Oncol.* 18, 181–191. [PubMed: 28007457]
282. Gill IS, Azzouzi AR, Emberton M, Coleman JA, Coeytaux E, Scherz A and Scardino PT (2018) Randomized Trial of Partial Gland Ablation with Vascular Targeted Phototherapy versus Active Surveillance for Low Risk Prostate Cancer: Extended Followup and Analyses of Effectiveness. *J. Urol* 200, 786–793. [PubMed: 29864437]
283. Bressler NM, Bressler SB and Fine L (1988) Age-related Macular Degeneration. *Surv. Ophthalmol* 32, 375–413. [PubMed: 2457955]
284. Prasad PS, Schwartz SD and Hubschman JP (2010) Age-related macular degeneration: Current and novel therapies. *Maturitas* 66, 46–50. [PubMed: 20219298]
285. Schmidt-Erfurth U and Hasan T (2000) Mechanisms of action of photodynamic therapy with verteporphin for the treatment of age-related macular degeneration. *Surv. Ophthalmol* 45, 195–214. [PubMed: 11094244]
286. Schmidt-Erfurth U, Hasan T, Gragoudas E, Michaud N, Flotte TJ and Birngruber R (1994) Vascular Targeting in Photodynamic Occlusion of Subretinal Vessels. *Ophthalmology* 101, 1953–1961. [PubMed: 7997334]
287. Kramer M, Miller JW, Michaud N, Moulton RS, Hasan T, Flotte TJ and Gragoudas ES (1996) Liposomal benzoporphyrin derivative verteporphin photodynamic therapy: Selective treatment of choroidal neovascularization in monkeys. *Ophthalmology* 103, 427–438. [PubMed: 8600419]
288. Group, T. of A. M. D. W. P. T. (TAP) S. (1999) Photodynamic Therapy of Subfoveal Choroidal Neovascularization in Age-related Macular Degeneration With Verteporphin: One-Year Results of 2 Randomized Clinical Trials—TAP Report 1. *JAMA Ophthalmol.* 117, 1329–1345.
289. >Groups, T. of A.-R. M. D. W. P. T. (TAP) and V. in P. T. (VIP) S. (2003) Photodynamic Therapy of Subfoveal Choroidal Neovascularization With Verteporphin: Fluorescein Angiographic Guidelines for Evaluation and Treatment—TAP and VIP Report No. 2. *JAMA Ophthalmol.* 121, 1253–1268.

290. Piao W, Hanaoka K, Fujisawa T, Takeuchi S, Komatsu T, Ueno T, Terai T, Tahara T, Nagano T and Urano Y (2017) Development of an azo-based photosensitizer activated under mild hypoxia for photodynamic therapy. *J. Am. Chem. Soc.* 139, 13713–13719. [PubMed: 28872304]
291. Busch TM, Wileyto EP, Emanuele MJ, Del Piero F, Marconato L, Glatstein E and Koch CJ (2002) Photodynamic Therapy Creates Fluence Rate-dependent Gradients in the Intratumoral Spatial Distribution of Oxygen. *Cancer Res.* 62, 7273 LP–7279. [PubMed: 12499269]
292. Feng L, Cheng L, Dong Z, Tao D, Barnhart TE, Cai W, Chen M and Liu Z (2017) Theranostic Liposomes with Hypoxia-Activated Prodrug to Effectively Destruct Hypoxic Tumors Post-Photodynamic Therapy. *ACS Nano* 11, 927–937. [PubMed: 28027442]
293. Albertella MR, Loadman PM, Jones PH, Phillips RM, Rampling R, Burnet N, Alcock C, Anthony A, Vjaters E, Dunk CR, Harris PA, Wong A, Lalani AS and Twelves CJ (2008) Hypoxia-selective targeting by the bioreductive prodrug AQ4N in patients with solid tumors: Results of a phase I study. *Clin. Cancer Res* 14, 1096–1104. [PubMed: 18281542]
294. Liu Y, Liu Y, Bu W, Cheng C, Zuo C, Xiao Q, Sun Y, Ni D, Zhang C, Liu J and Shi J (2015) Hypoxia Induced by Upconversion-Based Photodynamic Therapy: Towards Highly Effective Synergistic Bioreductive Therapy in Tumors. *Angew. Chemie - Int. Ed* 54, 8105–8109.
295. Marcu L and Olver I (2008) Tirapazamine: From Bench to Clinical Trials. *Curr. Clin. Pharmacol* 1, 71–79.
296. Jahanban-Esfahlan R, de la Guardia M, Ahmadi D and Yousefi B (2018) Modulating tumor hypoxia by nanomedicine for effective cancer therapy. *J. Cell. Physiol* 233, 2019–2031. [PubMed: 28198007]
297. Song X, Feng L, Liang C, Yang K and Liu Z (2016) Ultrasound Triggered Tumor Oxygenation with Oxygen-Shuttle Nanoperfluorocarbon to Overcome Hypoxia-Associated Resistance in Cancer Therapies. *Nano Lett.* 16, 6145–6153. [PubMed: 27622835]
298. Modery-Pawloski CL, Tian LL, Pan V and Sen Gupta A (2013) Synthetic Approaches to RBC Mimicry and Oxygen Carrier Systems. *Biomacromolecules* 14, 939–948. [PubMed: 23452431]
299. Zhou Z, Song J, Nie L and Chen X (2016) Reactive oxygen species generating systems meeting challenges of photodynamic cancer therapy. *Chem. Soc. Rev* 45, 6597–6626. [PubMed: 27722328]
300. Wan G, Chen B, Li L, Wang D, Shi S, Zhang T, Wang Y, Zhang L and Wang Y (2018) Nanoscaled red blood cells facilitate breast cancer treatment by combining photothermal/photodynamic therapy and chemotherapy. *Biomaterials* 155, 25–40. [PubMed: 29161627]
301. Vankayala R, Huang Y-K, Kalluru P, Chiang C-S and Hwang KC (2014) First Demonstration of Gold Nanorods-Mediated Photodynamic Therapeutic Destruction of Tumors via Near Infra-Red Light Activation. *Small* 10, 1612–1622. [PubMed: 24339243]
302. Gunaydin G, Turan IS, Yildiz D, Turksoy A and Akkaya EU (2018) A novel approach for fractional photodynamic therapy utilizing a photosensitizer with an additional 2 - pyridone module. *FEBS Open Bio* 8, 179.
303. Luo GF, Chen WH, Hong S, Cheng Q, Qiu WX and Zhang XZ (2017) A Self-Transformable pH-Driven Membrane-Anchoring Photosensitizer for Effective Photodynamic Therapy to Inhibit Tumor Growth and Metastasis. *Adv. Funct. Mater* 27, 1–13.
304. Andreev OA, Wyatt LC, Crawford T, Engelman DM, Reshetnyak YK and Moshnikova A (2018) Peptides of pHLIP family for targeted intracellular and extracellular delivery of cargo molecules to tumors. *Proc. Natl. Acad. Sci* 115, E2811–E2818. [PubMed: 29507241]
305. Yu M, Guo F, Wang J, Tan F and Li N (2015) Photosensitizer-Loaded pH-Responsive Hollow Gold Nanospheres for Single Light-Induced Photothermal/Photodynamic Therapy. *ACS Appl. Mater. Interfaces* 7, 17592–17597. [PubMed: 26248033]
306. Han K, Zhang WY, Zhang J, Lei Q, Wang SB, Liu JW, Zhang XZ and Han HY (2016) Acidity-Triggered Tumor-Targeted Chimeric Peptide for Enhanced Intra-Nuclear Photodynamic Therapy. *Adv. Funct. Mater* 26, 4351–4361.
307. Gao M, Fan F, Li D, Yu Y, Mao K, Sun T, Qian H, Tao W and Yang X (2017) Tumor acidity-activatable TAT targeted nanomedicine for enlarged fluorescence/magnetic resonance imaging-guided photodynamic therapy. *Biomaterials* 133, 165–175. [PubMed: 28437627]

308. Copolovici DM, Langel K, Eriste E and Langel Ü (2014) Cell-penetrating peptides: Design, synthesis, and applications. *ACS Nano* 8, 1972–1994. [PubMed: 24559246]
309. Pereira PMR, Korsak B, Sarmento B, Schneider RJ, Fernandes R and Tomé JPC (2015) Antibodies armed with photosensitizers: From chemical synthesis to photobiological applications. *Org. Biomol. Chem* 13, 2518–2529. [PubMed: 25612113]
310. Chang M-H, Pai C-L, Lai P-S, Chen Y-C, Hsu C-Y and Yu H-P (2018) Enhanced Antitumor Effects of Epidermal Growth Factor Receptor Targetable Cetuximab-Conjugated Polymeric Micelles for Photodynamic Therapy. *Nanomaterials* 8, 1–16.
311. Pereira PMR, Sarmento B, Fernandes R, Fernandes SRG and Tomé JPC (2019) Photoimmunoconjugates: novel synthetic strategies to target and treat cancer by photodynamic therapy. *Org. Biomol. Chem* 17, 2579–2593. [PubMed: 30648722]
312. Wat C, Towers GHN and Levy JG (1983) Photoimmunotherapy: treatment of animal tumors with tumor-specific monoclonal antibody-hematioporphyrin conjugates. *J. Immunol* 130, 1473–1377. [PubMed: 6185591]
313. Hamblin MR, Miller JL and Hasan T (1996) Effect of charge on the interaction of site-specific photoimmunoconjugates with human ovarian cancer cells. *Cancer Res.* 56, 5205–5210. [PubMed: 8912858]
314. Carcenac M, Dorvillius M, Garambois V, Glaussel F, Larroque C, Langlois R, Hynes NE, Van Lier JE and Pèlegri A (2001) Internalisation enhances photo-induced cytotoxicity of monoclonal antibody-phthalocyanine conjugates. *Br. J. Cancer* 85, 1787–1793. [PubMed: 11742503]
315. Vrouenraets MB, Visser GWM, Stewart FA, Stigter M, Oppelaar H, Postmus PE, Snow GB and Van Dongen GAMS (1999) Development of meta-tetrahydroxyphenylchlorin-monoclonal antibody conjugates for photoimmunotherapy. *Cancer Res.* 59, 1505–1513. [PubMed: 10197621]
316. Savellano MD and Hasan T (2003) Targeting Cells That Overexpress the Epidermal Growth Factor Receptor with Polyethylene Glycolated BPD Verteporfin Photosensitizer Immunoconjugates. *Photochem. Photobiol* 77, 431–439. [PubMed: 12733655]
317. Mitsunaga M, Ogawa M, Kosaka N, Rosenblum LT, Choyke PL and Kobayashi H (2011) Cancer cell-selective in vivo near infrared photoimmunotherapy targeting specific membrane molecules. *Nat. Med* 17, 1685–1691. [PubMed: 22057348]
318. Spring BQ, Abu-Yousif AO, Palanisami A, Rizvi I, Zheng X, Mai Z, Anbil S, Sears RB, Mensah LB, Goldschmidt R, Erdem SS, Oliva E and Hasan T (2014) Selective treatment and monitoring of disseminated cancer micrometastases in vivo using dual-function, activatable immunoconjugates. *Proc. Natl. Acad. Sci* 111, E933–E942. [PubMed: 24572574]
319. Ogawa M, Tomita Y, Nakamura Y, Lee M-J, Lee S, Tomita S, Nagaya T, Sato K, Yamauchi T, Iwai H, Kumar A, Haystead T, Shroff H, Choyke PL, Trepel JB, Kobayashi H, Ogawa M, Tomita Y, Nakamura Y, Lee M-J, Lee S, Tomita S, Nagaya T, Sato K, Yamauchi T, Iwai H, Kumar A, Haystead T, Shroff H, Choyke PL, Trepel JB and Kobayashi H (2017) Immunogenic cancer cell death selectively induced by near infrared photoimmunotherapy initiates host tumor immunity. *Oncotarget* 8, 10425–10436. [PubMed: 28060726]
320. Sato K, Ando K, Okuyama S, Moriguchi S, Ogura T, Totoki S, Hanaoka H, Nagaya T, Kokawa R, Takakura H, Nishimura M, Hasegawa Y, Choyke PL, Ogawa M and Kobayashi H (2018) Photoinduced Ligand Release from a Silicon Phthalocyanine Dye Conjugated with Monoclonal Antibodies: A Mechanism of Cancer Cell Cytotoxicity after Near-Infrared Photoimmunotherapy. *ACS Cent. Sci* 4, 1559–1569. [PubMed: 30555909]
321. Zhen Z, Tang W, Wang M, Zhou S, Wang H, Wu Z, Hao Z, Li Z, Liu L and Xie J (2017) Protein Nanocage Mediated Fibroblast-Activation Protein Targeted Photoimmunotherapy to Enhance Cytotoxic T Cell Infiltration and Tumor Control. *Nano Lett.* 17, 862–869. [PubMed: 28027646]
322. Chen X and Song E (2019) Turning foes to friends: targeting cancer-associated fibroblasts. *Nat. Rev. Drug Discov* 18, 99–115. [PubMed: 30470818]
323. Miao L, Lin CM and Huang L (2015) Stromal barriers and strategies for the delivery of nanomedicine to desmoplastic tumors. *J. Control. Release* 219, 192–204. [PubMed: 26277065]
324. Li L, Zhou S, Lv N, Zhen Z, Liu T, Gao S, Xie J and Ma Q (2018) Photosensitizer-Encapsulated Ferritins Mediate Photodynamic Therapy against Cancer-Associated Fibroblasts and Improve Tumor Accumulation of Nanoparticles. *Mol. Pharm* 15, 3595–3599. [PubMed: 29966416]

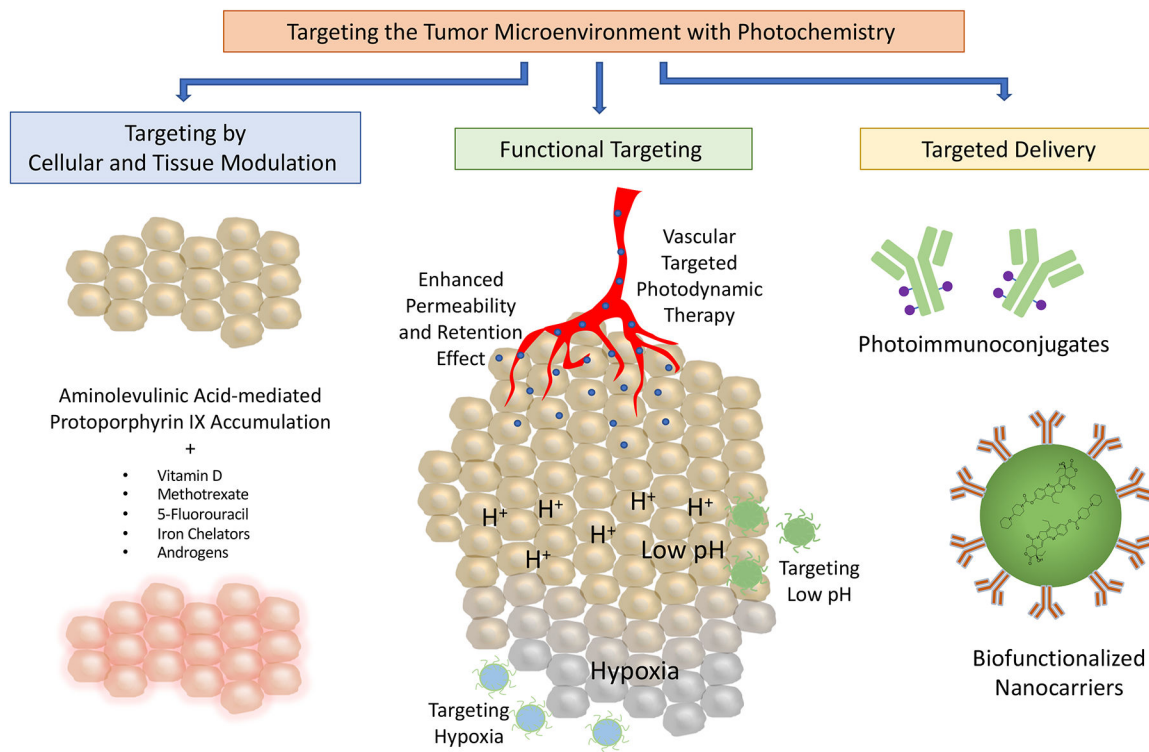
325. Huang HC, Pigula M, Fang Y and Hasan T (2018) Immobilization of Photo-Immunoconjugates on Nanoparticles Leads to Enhanced Light-Activated Biological Effects. *Small* 14, 1–11.
326. You H, Yoon HE, Jeong PH, Ko H, Yoon JH and Kim YC (2015) Pheophorbide-a conjugates with cancer-targeting moieties for targeted photodynamic cancer therapy. *Bioorganic Med. Chem* 23, 1453–1462.
327. Zhang Q, Cai Y, Li QY, Hao LN, Ma Z, Wang XJ and Yin J (2017) Targeted Delivery of a Mannose-Conjugated BODIPY Photosensitizer by Nanomicelles for Photodynamic Breast Cancer Therapy. *Chem. - A Eur. J* 23, 14307–14315.
328. García Calavia P, Chambrier I, Cook MJ, Haines AH, Field RA and Russell DA (2018) Targeted photodynamic therapy of breast cancer cells using lactose-phthalocyanine functionalized gold nanoparticles. *J. Colloid Interface Sci* 512, 249–259. [PubMed: 29073466]
329. Hayashi N, Kataoka H, Yano S, Tanaka M, Moriwaki K, Akashi H, Suzuki S, Mori Y, Kubota E, Tanida S, Takahashi S and Joh T (2014) A Novel Photodynamic Therapy Targeting Cancer Cells and Tumor-Associated Macrophages. *Mol. Cancer Ther* 14, 452–460. [PubMed: 25512617]
330. Tran TH, Nguyen HT, Phuong Tran TT, Ku SK, Jeong JH, Choi HG, Yong CS and Kim JO (2017) Combined photothermal and photodynamic therapy by hyaluronic acid-decorated polypyrrole nanoparticles. *Nanomedicine* 12, 1511–1523. [PubMed: 28573923]
331. Obaid G, Chambrier I, Cook MJ and Russell DA (2015) Cancer targeting with biomolecules: A comparative study of photodynamic therapy efficacy using antibody or lectin conjugated phthalocyanine-PEG gold nanoparticles. *Photochem. Photobiol. Sci* 14, 737–747. [PubMed: 25604735]
332. Kato T, Jin CS, Ujiie H, Lee D, Fujino K, Wada H, Hu H. pei, Weersink RA, Chen J, Kaji M, Kaga K, Matsui Y, Wilson BC, Zheng G and Yasufuku K (2017) Nanoparticle targeted folate receptor 1-enhanced photodynamic therapy for lung cancer. *Lung Cancer* 113, 59–68. [PubMed: 29110850]
333. Ma X, Qu Q and Zhao Y (2015) Targeted Delivery of 5-Aminolevulinic Acid by Multifunctional Hollow Mesoporous Silica Nanoparticles for Photodynamic Skin Cancer Therapy. *ACS Appl. Mater. Interfaces* 7, 10671–10676. [PubMed: 25974979]
334. Clement S, Chen W, Deng W and Goldys EM (2018) X-ray radiation-induced and targeted photodynamic therapy with folic acid-conjugated biodegradable nanoconstructs. *Int. J. Nanomedicine* 13, 3553–3570. [PubMed: 29950835]
335. Sebak AA, Gomaa IEO, ElMeshad AN and AbdelKader MH (2018) Targeted photodynamic-induced singlet oxygen production by peptide-conjugated biodegradable nanoparticles for treatment of skin melanoma. *Photodiagnosis Photodyn. Ther* 23, 181–189. [PubMed: 29885810]
336. Meyers JD, Cheng Y, Broome AM, Agnes RS, Schluchter MD, Margevicius S, Wang X, Kenney ME, Burda C and Basilion JP (2015) Peptide-targeted gold nanoparticles for photodynamic therapy of brain cancer. *Part. Part. Syst. Charact* 32, 448–457. [PubMed: 25999665]
337. Stuchinskaya T, Moreno M, Cook MJ, Edwards DR and Russell DA (2011) Targeted photodynamic therapy of breast cancer cells using antibody-phthalocyanine-gold nanoparticle conjugates. *Photochem. Photobiol. Sci* 10, 822–831. [PubMed: 21455532]
338. Broekgaarden M, Van Vught R, Oliveira S, Roovers RC, Van Bergen En Henegouwen PMP, Pieters RJ, Van Gulik TM, Breukink E and Heger M (2016) Site-specific conjugation of single domain antibodies to liposomes enhances photosensitizer uptake and photodynamic therapy efficacy. *Nanoscale* 8, 6490–6494. [PubMed: 26954515]
339. Komohara Y and Takeya M (2017) CAFs and TAMs: maestros of the tumour microenvironment. *J. Pathol* 241, 313–315. [PubMed: 27753093]
340. Liu FT and Rabinovich GA (2005) Galectins as modulators of tumour progression. *Nat. Rev. Cancer* 5, 29–41. [PubMed: 15630413]
341. Ghazarian H, Idoni B and Oppenheimer SB (2011) A glycobiology review: Carbohydrates, lectins and implications in cancer therapeutics. *Acta Histochem.* 113, 236–247. [PubMed: 20199800]
342. Zwicke GL, Ali Mansoori G and Jeffery CJ (2012) Utilizing the folate receptor for active targeting of cancer nanotherapeutics. *Nano Rev.* 3, 1–11.
343. Wang F, Li Y, Shen Y, Wang A, Wang S and Xie T (2013) The functions and applications of RGD in tumor therapy and tissue engineering. *Int. J. Mol. Sci* 14, 13447–13462. [PubMed: 23807504]

344. Zhao N, Qin Y, Liu H and Cheng Z (2017) Tumor-Targeting Peptides: Ligands for Molecular Imaging and Therapy. *Anticancer. Agents Med. Chem* 18, 74–86.
345. Li L and Huh KM (2014) Polymeric nanocarrier systems for photodynamic therapy. *Biomater. Res* 18, 1–14.
346. Gao L, Zhang C, Gao D, Liu H, Yu X, Lai J, Wang F, Lin J and Liu Z (2016) Enhanced Anti-Tumor Efficacy through a Combination of Integrin  $\alpha v \beta 6$ -Targeted Photodynamic Therapy and Immune Checkpoint Inhibition. *Theranostics* 6, 627–637. [PubMed: 27022411]
347. Pacheco-Soares C, Maftou-Costa M, DA Cunha Menezes Costa CG, DE Siqueira Silva C and Moraes KCM (2014) Evaluation of photodynamic therapy in adhesion protein expression. *Oncol. Lett* 8, 714–718. [PubMed: 25013490]
348. Noy R and Pollard JW (2014) Tumor-Associated Macrophages: From Mechanisms to Therapy. *Immunity* 41, 49–61. [PubMed: 25035953]
349. Afik R, Zigmond E, Vugman M, Klepfish M, Shimshoni E, Pasmanik-Chor M, Shenoy A, Bassat E, Halpern Z, Geiger T, Sagi I and Varol C (2016) Tumor macrophages are pivotal constructors of tumor collagenous matrix. *J. Exp. Med* 213, 2315–2331. [PubMed: 27697834]
350. Satelli A and Li S (2011) Vimentin in cancer and its potential as a molecular target for cancer therapy. *Cell. Mol. Life Sci* 68, 3033–3046. [PubMed: 21637948]
351. Werb Z and Lu P (2015) The Role of Stroma in Tumor Development. *Cancer J. (United States)* 21, 250–253.

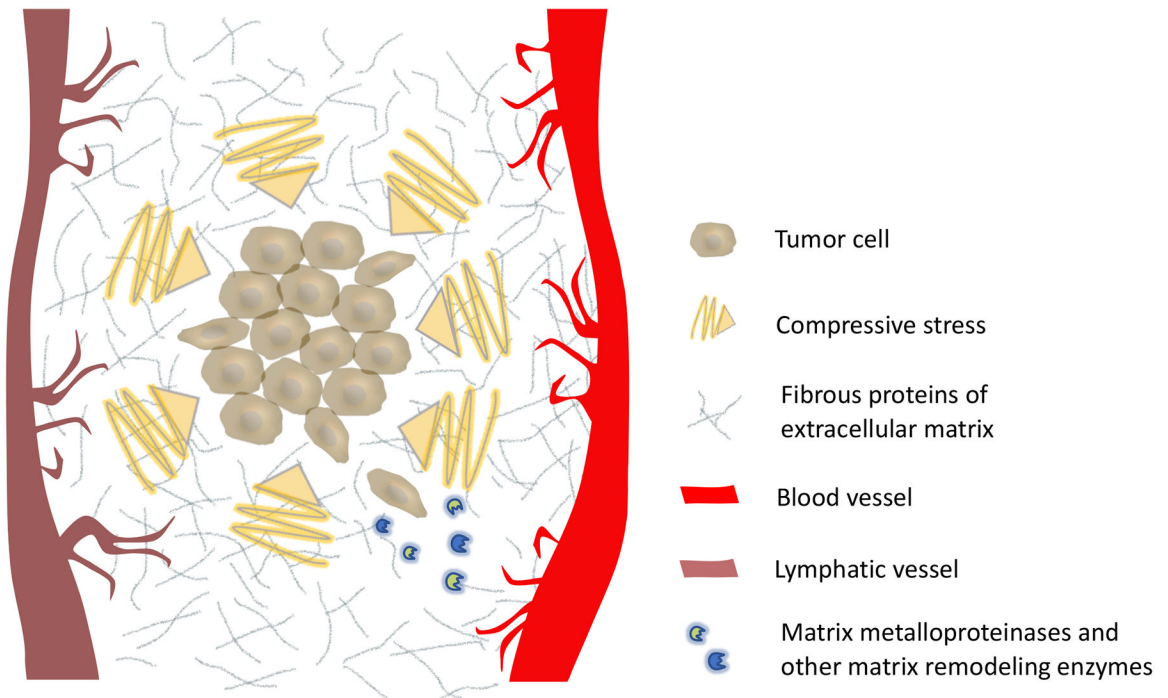


**Figure 1.**

The tumor microenvironment is composed of cellular and noncellular components, as well as various mechanical stresses, that can inhibit or promote tumor growth and survival. These stromal components and mechanical stresses are described in the section on the tumor microenvironment as a target for cancer treatment.

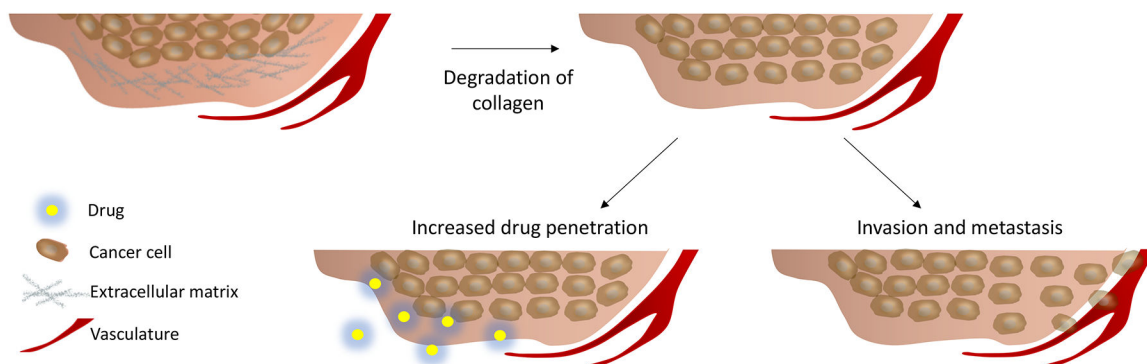


**Figure 2.** Categories of targeted photodynamic therapy that exploit cellular, molecular, and mechanical features of the tumor microenvironment: targeting by cellular and tissue modulation, functional targeting and targeted delivery.



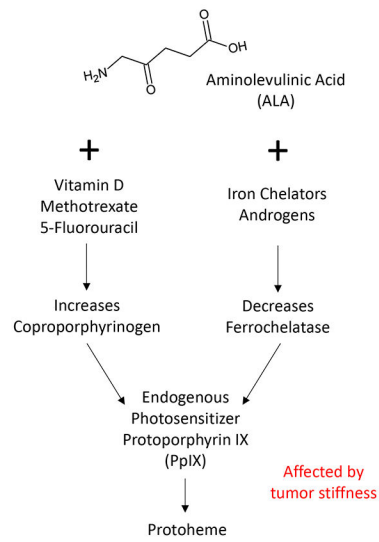
**Figure 3.**

The stiff extracellular matrix in the tumor microenvironment contributes to the generation of compressive stress on tumors. Compressive stress can inhibit tumor growth, while simultaneously activating invasive behavior. While dense, fibrous extracellular matrix impedes motility, invading cancer cells use matrix metalloproteinases, or other matrix remodeling enzymes, to create migratory paths (50).

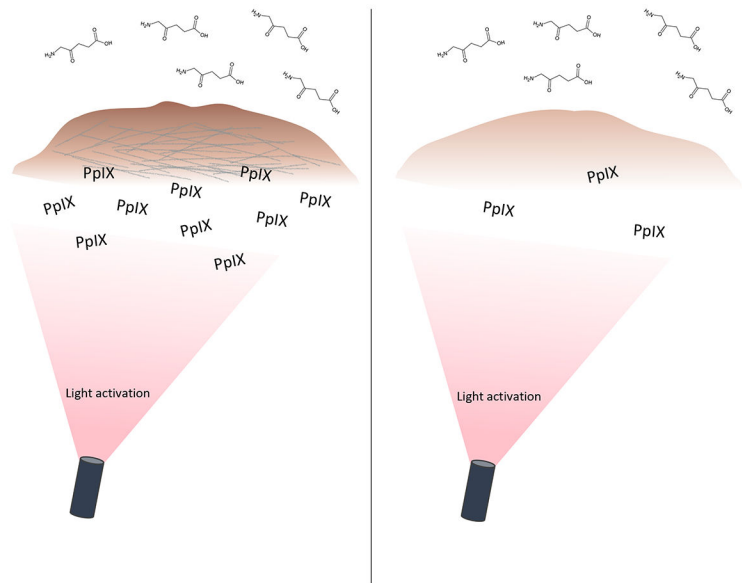


**Figure 4.** Extracellular matrix degradation can increase drug penetration into tumor tissues, though this degradation can also facilitate cancer cell invasion and metastasis.

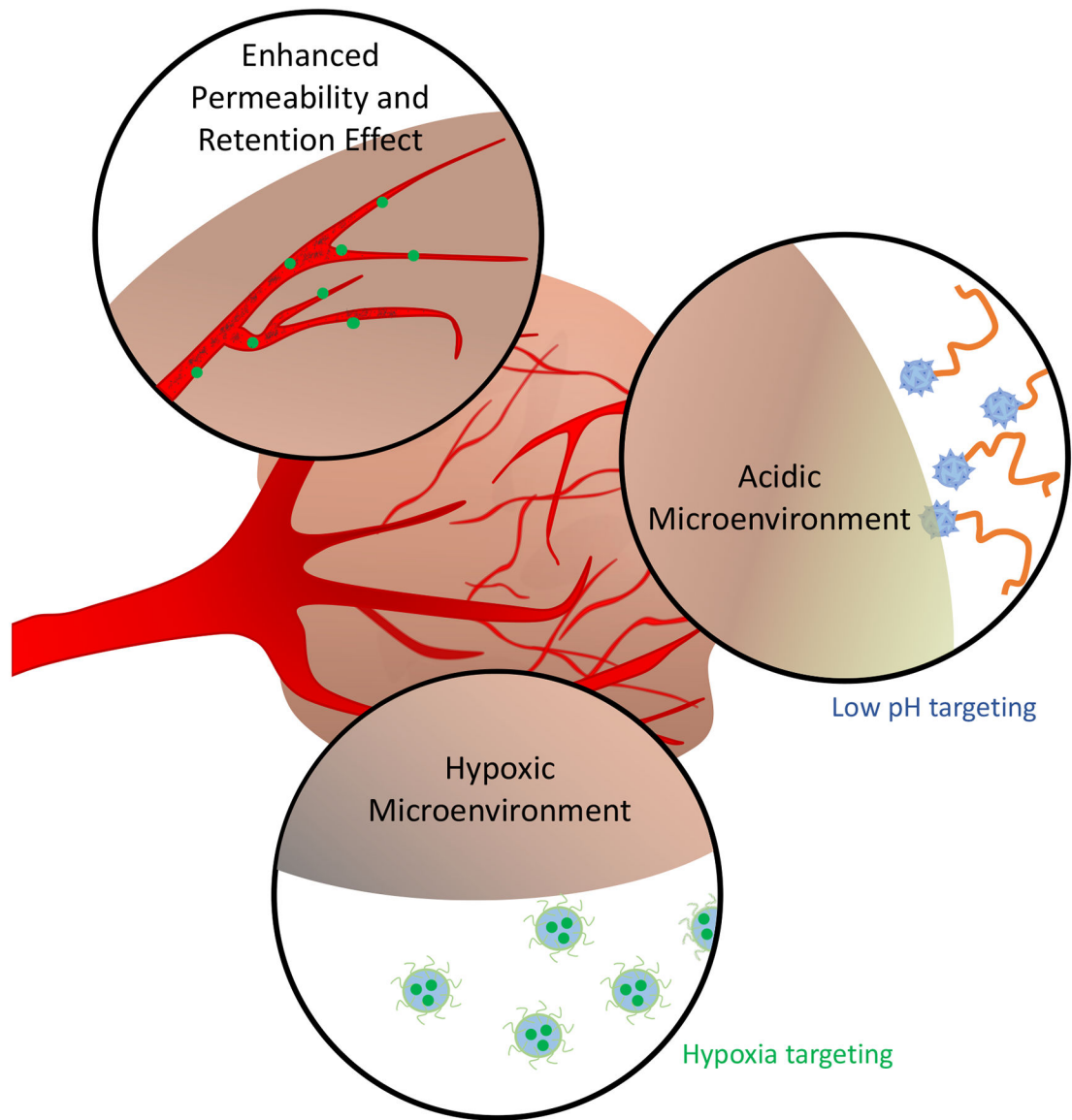
## a) Targeting by Cellular and Tissue Modulation



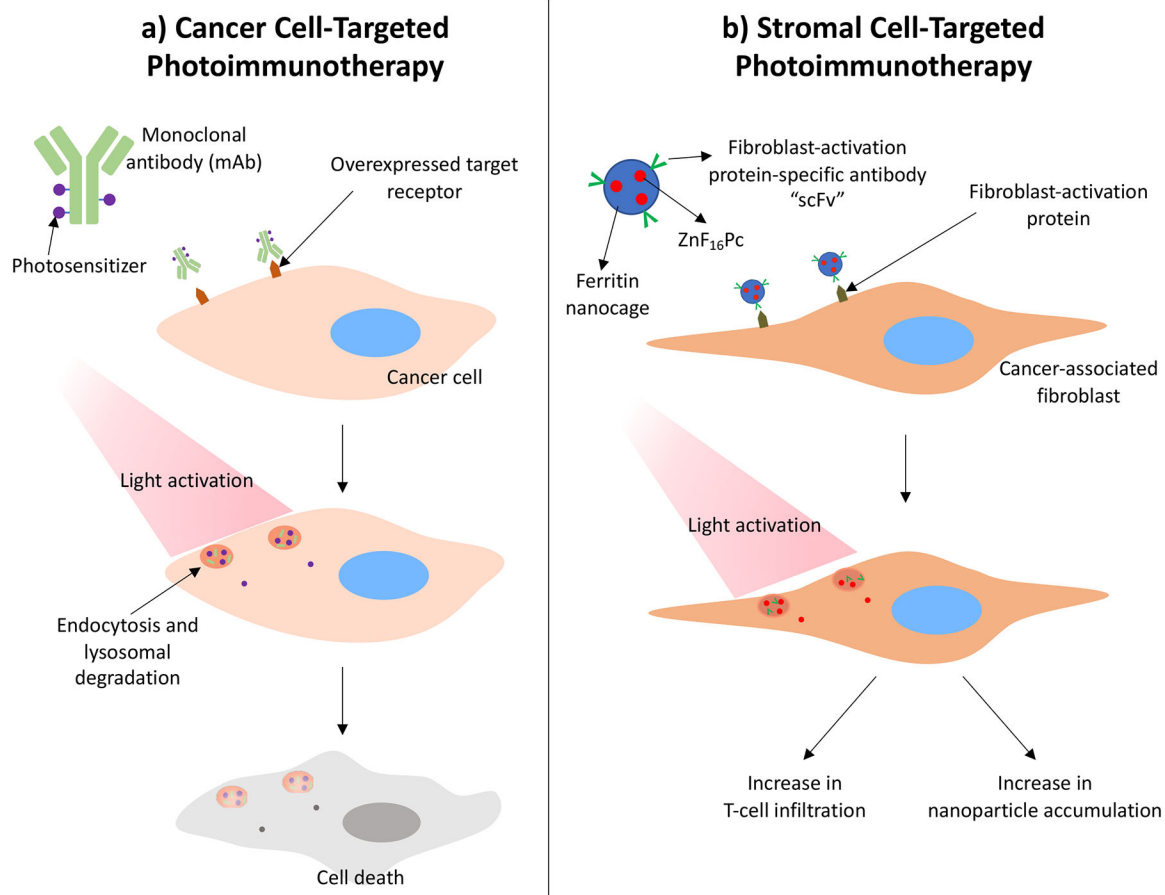
## b) Matrix Stiffness Affects Protoporphyrin IX (PpIX) Production

**Figure 5.**

a) Summary of the pathways involved in targeting by cellular and tissue modulation, and b) increased PpIX accumulation with higher substrate stiffness in glioma cells (13).



**Figure 6.** Characteristics of the tumor microenvironment that are exploited for functional targeting.

**Figure 7.**

a) Schematic of photoimmunoconjugate uptake by a cancer cell. The antibody binds to the target cell and is internalized by receptor-mediated endocytosis. At certain photosensitizer:antibody ratios, lysosomal degradation mechanisms can be leveraged to dequench the photosensitizer, allowing for light activation. Following light activation, reactive molecular species are generated to induce cytotoxicity in target cell. b) Cancer-associated fibroblast-targeted photoimmunotherapy and the associated effects on the tumor microenvironment (321, 324).

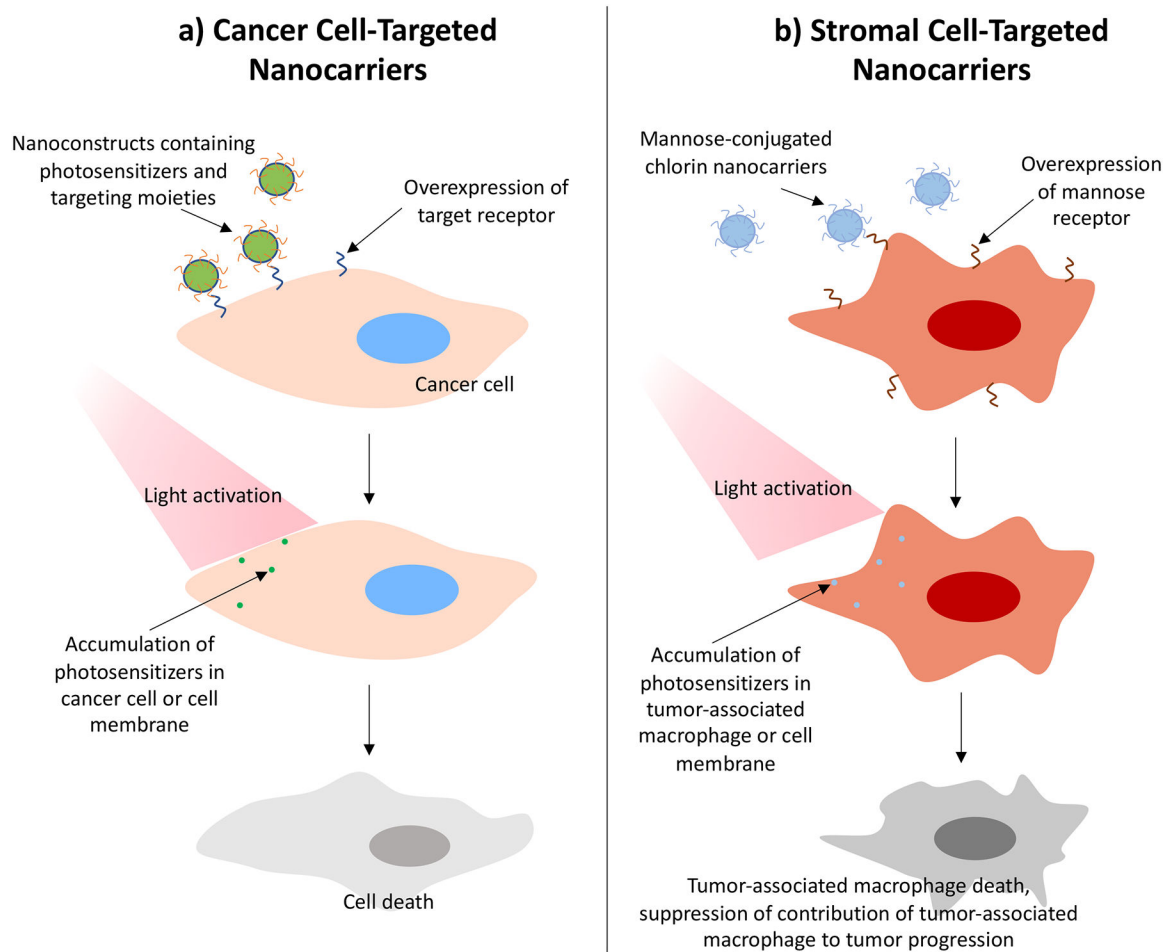


**Figure 8.** Depiction of the interactions between targeted photoactivatable nanocarriers and a) cancer cells or b) tumor-associated macrophages (329).

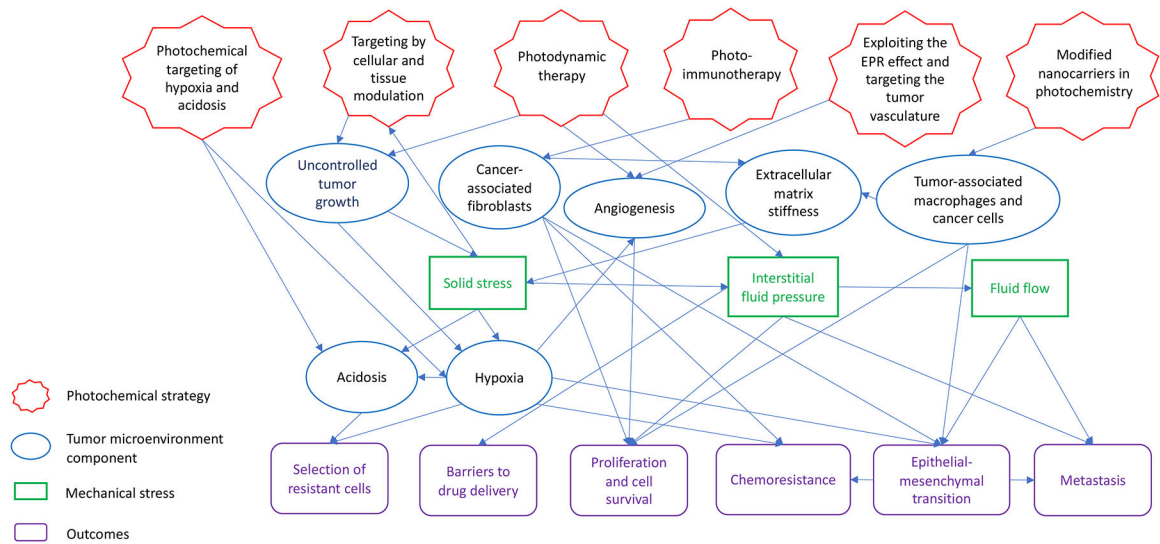


**Figure 9.**

The web of interactions between the components and mechanical stresses of the tumor microenvironment, and how they contribute to the development of treatment resistance and cancer progression. Photodynamic therapy can be used to alter these outcomes.

**Table 1.**

Photosensitizers that are commonly used in the clinic and in preclinical studies.

Photosensitizer	Family	Generation	Localization	References
HpD	Porphyrin	1 <sup>st</sup>	Multiple organelles and cell membrane	(160, 170)
BPD	Porphyrin	2 <sup>nd</sup>	Mitochondria and ER, or vasculature depending on the photosensitizer-light interval	(161, 162)
NPe6	Chlorin	2 <sup>nd</sup>	Lysosomes	(132, 168)
Tookad	Bacteriochlorin	2 <sup>nd</sup>	Tumor vasculature	(163)
Photofrin	Porphyrin	1 <sup>st</sup>	Plasma membrane and Golgi apparatus	(164)
Foscan	Chlorin	2 <sup>nd</sup>	ER and Golgi apparatus	(165, 166)
ZnPc	Phthalocyanine	2 <sup>nd</sup>	Mitochondria and lysosomes	(167)
ALA	Porphyrin	2 <sup>nd</sup>	PpIX produced in mitochondria, some relocalizes to the plasma membrane and lysosomes	(169)

Author Manuscript

Author Manuscript

Author Manuscript

Author Manuscript

**Table 2.**

A summary of differentiating agents, along with the target diseases.

Differentiating Agent	PpIX Accumulation Mechanism	Diseases Treated	References
Vitamin D	Increases coproporphyrinogen	breast cancer, squamous cell carcinoma, melanoma, actinic keratosis, prostate cancer	(191, 192, 203, 211–213)
5-Fluorouracil	Increases coproporphyrinogen	actinic keratoses, melanoma, cervical cancer, mucosal lesions, intraepithelial squamous cell carcinoma	(193–197)
Iron Chelators	Decreases ferrochelatase	lung and normal fibroblasts, epidermal, pancreatic, bladder, colon, urothelial and skin carcinoma, adenocarcinoma carcinomas, basal cell carcinoma, solar keratoses, and lesions of Bowen's disease	(198–202, 204–210)
Androgens	Decreases ferrochelatase	prostate cancer, breast cancer	(211, 214)
Methotrexate	Increases coproporphyrinogen	prostate cancer, buccal precancers, cervical cancer, head and neck cancer	(215–217)

Author Manuscript

Author Manuscript

Author Manuscript

Author Manuscript

**Table 3.**

A summary of various types of targeting moieties and details regarding their use.

Targeting moiety	Nanoparticle or molecule to which the moiety is conjugated	Target receptor	Target disease	References
Folic acid	Porphyrin-lipid nanoparticles (porphysomes), Hollow mesoporous silica nanoparticles, PLGA nanoparticles,	Folate receptor	Lung cancer, Skin cancer, Colorectal cancer	(332–334)
Peptides	Gold nanoparticles, PGLA nanoparticles	T antigen, $\alpha_v\beta_3$ , $\alpha_v\beta_6$ , EGFR	Colon cancer, Breast cancer, Melanoma, Glioma	(331, 335, 336)
Antibodies	Gold nanoparticles, Liposomes, PLGA nanoparticles	HER-2, EGFR	Colon cancer, Breast cancer, Epidermoid carcinoma, Ovarian cancer, Glioblastoma	(325, 331, 337, 338)
Carbohydrates	Chlorin, Nanomicelles, Gold nanoparticles, PLGA nanoparticles	Mannose receptor, Galectin-1, CD44	Gastric cancer, Colon cancer, Breast cancer, Oral squamous cell carcinoma	(327–330)